

# Reliability assessment of craniofacial and airway measurements: a comparative study between multidetector computed tomography and cone-beam computed tomography

Jui-Sheng Sun<sup>a</sup>; Min-Chih Hung<sup>b</sup>; Chi-Yeh Hsieh<sup>c</sup>; Shih-Ying Lin<sup>d</sup>; Han-Cheng Tai<sup>e</sup>; Jenny Zwei-Chiang Chang<sup>f</sup>

## ABSTRACT

**Objectives:** To compare the intra- and inter-examiner reliability of multidetector computed tomography (MDCT) and cone-beam computed tomography (CBCT) using Amira and Dolphin software analyses for craniofacial/airway measurements by six examiners.

**Materials and Methods:** Five adults and one dry skull with CBCT and MDCT scan files were duplicated and randomly numbered. Six orthodontic residents imported these files into two software programs, oriented the images, set thresholds, and performed 26 measurements. Intra- and inter-examiner reliabilities were determined by using intraclass correlation coefficient (ICC) and presented with scatterplots.

**Results:** Variables including anterior nasal width, posterior nasal width, frontomaxillary suture right-to-left, inner nasal contour point right-to-left, and minimum cross-sectional area in the oropharynx showed “moderate” to “substantial” intra- or inter-examiner agreement. Amira provided relatively reliable airway assessment, while Dolphin showed standard deviations 10 to 30 times larger for volumetric airway measurements. MDCT scans significantly reduced airway volume/area measurements compared to CBCT, except for intraoral airway volume.

**Conclusions:** Unreliable skeletal measurements and low reliability of Dolphin for airway analysis discourage using CT to quantitatively correlate changes in craniofacial structures with airway dimensions. (*Angle Orthod.* 2025;95:57–77.)

**KEY WORDS:** CBCT; MDCT; Reliability; ICC; Airway

## INTRODUCTION

Multi-detector (multi-slice) computed tomography (MDCT; MSCT) and cone-beam CT (CBCT) are prevalent CT technologies for head and neck evaluation,

albeit with distinct image-acquisition processes (including beam shape, x-ray generator, and detecting system).<sup>1</sup> Popularity of CBCT in maxillofacial imaging stems from its lower radiation dose, cost-effectiveness, and ease of installation. Applications

---

The first two authors contributed equally to this work.

<sup>a</sup> Visiting Staff, Department of Orthopedic Surgery, En Chu Kong Hospital, New Taipei City; and Professor, Department of Orthopedic Surgery, College of Medicine, National Taiwan University, Taipei, Taiwan.

<sup>b</sup> Visiting Staff, Department of Dentistry, National Taiwan University Hospital, Taipei, Taiwan.

<sup>c</sup> Postgraduate Student, School of Dentistry, College of Medicine, National Taiwan University, Taipei, Taiwan.

<sup>d</sup> Visiting Staff, Department of Dentistry, MacKay Memorial Hospital, Taipei, Taiwan.

<sup>e</sup> Visiting Staff, Department of Orthopedic Surgery, En Chu Kong Hospital, New Taipei City, Taiwan.

<sup>f</sup> Visiting Staff, Department of Dentistry, National Taiwan University Hospital, Taipei; and Associate Professor, School of Dentistry, College of Medicine, National Taiwan University, Taipei, Taiwan.

Corresponding author: Dr Jenny Zwei-Chiang Chang, School of Dentistry, College of Medicine, National Taiwan University, 1 Chang-De Street, Taipei 10046, Taiwan  
(e-mail: jennyzc@ms3.hinet.net)

Accepted: July 2024. Submitted: February 2024.

Published Online: September 25, 2024

© 2025 by The EH Angle Education and Research Foundation, Inc.

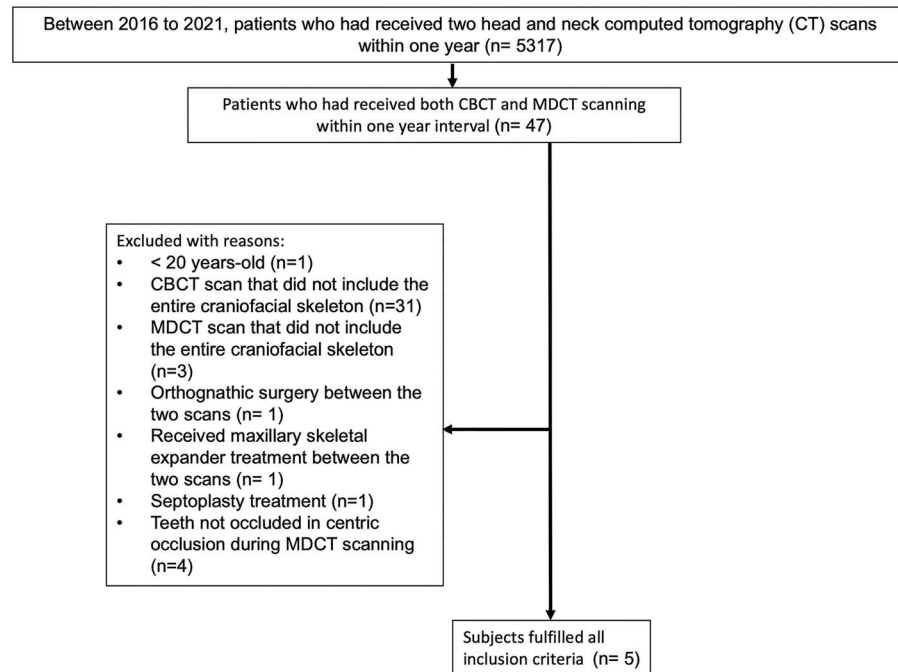


**Figure 1.** Subject screening flow chart.

extend to various medical fields, including orthodontics,<sup>2</sup> where it aids in assessing upper airway morphology, treatment effects, and disorders such as obstructive sleep apnea (OSA).<sup>3</sup> Concerns about cumulative radiation doses from repeated CBCT scans underscore the need for justifying routine use.<sup>4</sup>

MDCT quantifies radiodensity using the Hounsfield scale (HU) and provides absolute value for each tissue type. Due to inherent CBCT acquisition limitations,<sup>5</sup> most studies question the ability to convert CBCT gray values (GV) to MDCT HU.<sup>6</sup> Many CBCT manufacturers do not calibrate GV along a pseudo-HU scale and, even after recalibration, significant errors persist in quantitative CBCT GV use.<sup>7</sup> MDCT excels in contrast detectability, discerning contrast at about 1 HU, while CBCT typically discerns contrast within a 10 HU range, limiting its ability to distinguish between different soft tissue structures. Yamashina et al. found CBCT produced distinct CT values from MDCT for air, water, and soft tissues.<sup>8</sup> Nevertheless, accurate measurement by CBCT of air spaces in a phantom<sup>8</sup> suggests potential precision in oropharyngeal airway dimension assessment.

In craniofacial studies using human cadaver/skull or phantom/prototype, most research found no significant difference between physical linear measurements and those obtained through MDCT and CBCT scans.<sup>9–11</sup> However, Naser and Mehr reported differences in linear measurements on hemi-mandible specimens,<sup>12</sup> and

Chen et al. found variations in volumetric and cross-sectional area measurements using different MDCT and CBCT scanners.<sup>13</sup> Since these studies used stationary objects, reported accuracy may be higher than in clinical scenarios, in which longer acquisition time by CBCT (20 to 40 seconds) increases motion artifact risk compared to MDCT scans acquired in a single breath.

Given inherent weaknesses of CBCT and ongoing interest in clinical research, determining its reliability as a quantitative airway assessment tool is crucial. A systematic review on upper pharyngeal airway assessment using CBCT identified only five high-quality studies out of 42,<sup>14</sup> with concerns about overrated reliability due to a limited number of studies evaluating interexaminer reliability and the absence of manual orientation of scanned images. Previous evidence suggests the obscurity of reliability of CBCT in quantitative measurements, prompting the present study to compare intra- and inter-examiner reliability of MDCT and CBCT using two software programs (Amira and Dolphin) for craniofacial/airway parameters.

## MATERIALS AND METHODS

### Samples and Exposure

This retrospective study, approved by the Research Ethics Committee of National Taiwan University Hospital (approval number: 202201101RINA), utilized data from patients who underwent two head and neck CT scans between 2016 and 2021, sourced from the National

**Table 1.** Definition of 26 Skeletal and Airway Variables (Including Linear, Angular, Area, and Volumetric Measurements)

Measurement	Definition
Linear measurements on the orthogonal planes	
Anterior nasal width (ANW) (unit: millimeter; mm)	Locating sagittal slice at midsagittal plane and coronal slice passing through nasion; on coronal view, the horizontal measurement of the line connecting the deepest concavity on the bilateral walls of the nasal cavity. (Modified from Pangrazio-Kulbersh et al., 2012, and Venezia et al., 2022)
Anterior nasal floor width (ANFW) (unit: millimeter; mm)	Locating sagittal slice at midsagittal plane and coronal slice passing through nasion; on coronal view, the horizontal measurement of the line connecting the transitional concavity from the bilateral walls of the nasal cavity to the floor of nose. (Modified from Pangrazio-Kulbersh et al., 2012, and Venezia et al., 2022)
Posterior nasal width (PNW) (unit: millimeter; mm)	Locating sagittal and coronal slices passing through the furcation of maxillary right first molar; on coronal view, the horizontal measurement of the widest superior transverse portion of the nasal aperture. (Modified from Pangrazio-Kulbersh et al., 2012 and Venezia et al., 2022)
Posterior nasal floor width (PNFW) (unit: millimeter; mm)	Locating sagittal and coronal slices passing through the furcation of maxillary right first molar; on coronal view, the horizontal measurement of the lowest transverse portion of the nasal aperture. (Modified from Pangrazio-Kulbersh et al., 2012, and Venezia et al., 2022)
External maxillary width (EMW) (unit: millimeter; mm)	Locating sagittal and coronal slices passing through the furcation of maxillary right first molar; on coronal view, the horizontal measurement of the line connecting the depth of concavity of the lateral walls of maxillary sinuses. (Modified from Kavand et al., 2019)
Palatal width (PW) (unit: millimeter; mm)	Locating sagittal and coronal slices passing through the furcation of maxillary right first molar; on coronal view, the horizontal measurement of the line connecting the junctions of the hard palate and lingual alveolar bone (Modified from Kavand et al., 2019)
Intermolar width at the first molar palatal apex level (Inter-Mpa) (unit: millimeter; mm)	Locating sagittal and coronal slices passing through the furcation of maxillary right first molar; on coronal view, the horizontal measurement of the line connecting the apices of the right and left maxillary first molars. (Modified from Kavand et al., 2019)
Intermolar width at the first molar central fossa level (Inter-Mcf) (unit: millimeter; mm)	Locating sagittal and coronal slices passing through the furcation of maxillary right first molar; on coronal view, the horizontal measurement of the line connecting the central fossae of the right and left maxillary first molars. (Modified from Kavand et al., 2019)
Linear measurements on the three-dimensional (3D) surface rendering images	
Zygomaticotemporal suture upper right to left (ZTUR-l) (unit: millimeter; mm)	Distance between the right and left upper borders of the zygomaticotemporal suture. (Modified from Yilmaz and Kucukkeles, 2015)
Frontomaxillary suture right to left (FMR-l) (unit: millimeter; mm)	Distance between the right and left inner borders of the frontomaxillary suture. (Modified from Cho et al., 2022, and Angelieri et al., 2017)
Frontozygomatic right to left (FZ r-l) (unit: millimeter; mm)	Distance between the right and left inner borders of the frontozygomatic suture. (Modified from Cho et al., 2022)
Inner nasal contour point right to left (INCR-l) (unit: millimeter, mm)	Distance between the right and left points on the most curved anterior border of the aperture piriformis. (Modified from Yilmaz and Kucukkeles, 2015)
Zygomatimaxillary upper right to left (ZMUR-l) (unit: millimeter, mm)	Distance between the right and left upper borders of the zygomatimaxillary suture. (Modified from Yilmaz and Kucukkeles, 2015)
Zygomatimaxillary lower right to left (ZMLR-l) (unit: millimeter, mm)	Distance between the right and left lower borders of the zygomatimaxillary suture. (Modified from Yilmaz and Kucukkeles, 2015)
Lateral cephalometric analysis	
Sella-Nasion-subspinale angle (SNA) (unit: degree)	On CT-derived lateral cephalogram, the measurement of angle from sella to nasion to subspinale point.
Sella-Nasion-supramentale angle (SNB) (unit: degree)	On CT-derived lateral cephalogram, the measurement of angle from sella to nasion to supramentale point.
Sella-Nasion-Gonion-Gnathion angle (SNGoGn) (unit: degree)	On CT-derived lateral cephalogram, the measurement of angle formed between gonion-gnathion (GoGn) line and sella-nasion (SN) line.
Lordosis angle (L) (unit: degree)	On CT-derived lateral cephalogram, the measurement of angle formed between sella-nasion (SN) line and the plane connecting through the most superior-posterior extremity of the odontoid process of the second cervical vertebrae (Cv2ig) and the most inferior-posterior point on the body of the second cervical vertebrae (Cv2ip). (Almuzian et al., 2018)

**Table 1.** Continued

Measurement	Definition
Condylion to Point A (Co-A) (unit: millimeter; mm)	Distance between condylion (the superior-most point on the head of the mandibular condyle) and subspinale point.
Condylion to Gnathion (Co-Gn) (unit: millimeter; mm)	Distance between condylion (the superior-most point on the head of the mandibular condyle) and gnathion.
Airway analysis	
Total oropharynx height (TOH) (unit: millimeter; mm)	Locating sagittal slice at mid-sagittal plane and axial slice at palatal plane; on sagittal view, the vertical measurement between upper and lower boundaries. (Upper boundary: plane parallel to Frankfort horizontal plane passing through posterior nasal spine and extended to the posterior wall of the pharynx; lower boundary: plane parallel to Frankfort horizontal plane connecting the base of the epiglottis) (Modified from Guijarro-Martínez and Swennen, 2013)
Intraoral airway volume (IAV) (unit: cubic millimeter; mm <sup>3</sup> )	The airway volume of between the palate and the tongue. (Iwasaki et al., 2019)
Nasopharyngeal airway volume (NAV) (unit: cubic millimeter; mm <sup>3</sup> )	Locating sagittal slice at midsagittal plane and axial slice at palatal plane (parallel to Frankfort horizontal passing through posterior nasal spine); the space between the soft tissue contour of the pharyngeal walls (upper and posterior boundaries) and lateral walls (lateral boundary), the frontal plane perpendicular to Frankfort horizontal passing through posterior nasal spine (anterior boundary), and palatal plane extended to the posterior wall of the pharynx (lower boundary) (Modified from Guijarro-Martínez and Swennen, 2013)
Oropharyngeal airway volume (OAV) (unit: cubic millimeter; mm <sup>3</sup> )	Locating sagittal slice at mid-sagittal plane and axial slice at palatal plane (parallel to Frankfort horizontal passing through posterior nasal spine); the space between the soft tissue contour of the pharyngeal wall (posterior boundary) and lateral walls (lateral boundary), the frontal plane perpendicular to Frankfort horizontal passing through posterior nasal spine (anterior boundary), the palatal plane extended to the posterior wall of the pharynx (upper boundary), and the plane parallel to Frankfort horizontal passing through the most anterior-inferior point of the body of third cervical vertebrae (lower boundary). (Modified from Guijarro-Martínez and Swennen, 2013)
Hypopharyngeal airway volume (HAV) (unit: cubic millimeter; mm <sup>3</sup> )	Locating sagittal slice at midsagittal plane and axial slice at palatal plane (parallel to Frankfort horizontal passing through posterior nasal spine); the space between the soft tissue contour of the pharyngeal wall (posterior boundary) and lateral walls (lateral boundary), the frontal plane perpendicular to Frankfort horizontal passing through posterior nasal spine (anterior boundary), the plane parallel to Frankfort horizontal passing through the most anterior-inferior point of the body of third cervical vertebrae (upper boundary), and Plane parallel to FH connecting the base of the epiglottis to the most anterior-inferior point of the body of fourth cervical vertebrae (lower boundary). (Modified from Guijarro-Martínez and Swennen, 2013)
Minimum cross-sectional area in oropharynx (MCA) (unit: square millimeter; mm <sup>2</sup> )	Locating sagittal slice at mid-sagittal plane and axial slice at palatal plane; automatically detected by software once the boundaries determined (upper boundary: plane parallel to Frankfort horizontal plane passing through posterior nasal spine and extended to the posterior wall of the pharynx; lower boundary: plane parallel to Frankfort horizontal passing through the most anterior-inferior point of the body of third cervical vertebrae; anterior boundary: the frontal plane perpendicular to Frankfort horizontal passing through posterior nasal spine; posterior boundary: soft tissue contour of the pharyngeal wall; lateral boundary: soft tissue contour of the pharyngeal lateral walls). (Modified from Guijarro-Martínez and Swennen, 2013)

Taiwan University Hospital-integrative Medical Database (NTUH-iMD). Inclusion criteria were: adults with both CBCT and MSCT scans within a year, and no head and neck treatment between scans. All CBCT images used were acquired by using 3D Accuitomo 170 (J.Morita MFG. Corp., Kyoto, Japan) with specified settings: 90 kVP, 5 mA, 17 × 12 cm, 0.25 mm, and exposure time of 35 seconds with two consecutive scans. MDCT images

used were acquired by using Somatom Definition AS (Siemens Medical Solutions, Malvern, Pennsylvania, USA): 120 kVP, 260 mA, 1.2 mm, 512 × 512, and exposure time of 0.5 seconds. Exclusion criteria included: age under 20 years, incomplete craniomaxillofacial skeleton coverage, non-occluded teeth in centric relation, or the use of different CT scanner models. Only five subjects fulfilled the inclusion criteria. The sampling flow

**Table 2.** Intra-examiner Reliabilities Estimated by Intraclass Correlation Coefficients (ICCs) for Repeated Measurements on Multidetector Computed Tomography (MDCT) Images Using Amira

MDCT × Amira	Variable	Examiner A ICC (95% CI)	Examiner B ICC (95% CI)	Examiner C ICC (95% CI)	Examiner D ICC (95% CI)	Examiner E ICC (95% CI)	Examiner F ICC (95% CI)
Linear measurements on the orthogonal planes	ANW	0.859 (0.280, 0.984)*	0.953 (0.698, 0.995)*	0.933 (0.591, 0.993)*	0.931 (0.584, 0.992)*	0.887 (0.387, 0.987)*	0.989 (0.920, 0.999)*
	ANFW	0.947 (0.665, 0.994)*	0.979 (0.853, 0.998)*	0.947 (0.664, 0.994)*	0.973 (0.816, 0.997)*	0.972 (0.812, 0.997)*	0.994 (0.953, 0.999)*
	PNW	0.737 (0.056, 0.968)*	0.837 (0.207, 0.981)*	0.871 (0.325, 0.985)*	0.803 (0.107, 0.977)*	0.916 (0.512, 0.991)*	0.970 (0.798, 0.997)*
	PNFW	0.967 (0.778, 0.996)*	0.946 (0.658, 0.994)*	0.958 (0.724, 0.995)*	0.942 (0.638, 0.994)*	0.978 (0.849, 0.998)*	0.989 (0.921, 0.999)*
	EMW	0.969 (0.792, 0.997)*	0.993 (0.950, 0.999)*	0.989 (0.922, 0.999)*	0.998 (0.988, 1.000)*	0.981 (0.870, 0.998)*	0.996 (0.972, 1.000)*
	PW	0.952 (0.744, 0.993)*	0.956 (0.762, 0.994)*	0.965 (0.807, 0.995)*	0.957 (0.767, 0.994)*	0.969 (0.827, 0.995)*	0.992 (0.954, 0.999)*
	Inter-Mpa	0.940 (0.687, 0.991)*	0.984 (0.909, 0.998)*	0.975 (0.858, 0.996)*	0.986 (0.918, 0.998)*	0.981 (0.893, 0.997)*	0.994 (0.966, 0.999)*
	Inter-Mcf	0.994 (0.953, 0.999)*	0.989 (0.920, 0.999)*	0.994 (0.958, 0.999)*	0.992 (0.945, 0.999)*	0.987 (0.906, 0.999)*	0.995 (0.961, 0.999)*
Linear measurements on the three- dimensional (3D) surface rendering images	ZTUR-l	0.996 (0.978, 0.999)*	0.998 (0.985, 1.000)*	0.996 (0.976, 0.999)*	0.998 (0.989, 1.000)*	0.998 (0.985, 1.000)*	0.999 (0.999, 1.000)*
	FMR-l	0.890 (0.401, 0.988)*	0.984 (0.889, 0.998)*	0.955 (0.709, 0.995)*	0.989 (0.921, 0.999)*	0.920 (0.529, 0.991)*	0.995 (0.965, 0.999)*
	FZR-l	0.987 (0.926, 0.998)*	0.990 (0.942, 0.999)*	0.987 (0.926, 0.998)*	0.996 (0.976, 0.999)*	0.994 (0.963, 0.999)*	0.998 (0.988, 1.000)*
	INCr-l	0.955 (0.759, 0.993)*	0.962 (0.794, 0.995)*	0.960 (0.780, 0.994)*	0.980 (0.888, 0.997)*	0.963 (0.797, 0.995)*	0.987 (0.926, 0.998)*
	ZMUR-l	0.977 (0.788, 0.998)*	0.990 (0.901, 0.999)*	0.984 (0.853, 0.999)*	0.984 (0.855, 0.999)*	0.994 (0.942, 1.000)*	0.998 (0.981, 1.000)*
Lateral cephalometric analysis	ZMLr-l	0.977 (0.843, 0.998)*	0.970 (0.796, 0.997)*	0.978 (0.849, 0.998)*	0.977 (0.839, 0.997)*	0.978 (0.848, 0.998)*	0.964 (0.764, 0.996)*
	SNA	0.989 (0.938, 0.998)*	0.979 (0.882, 0.997)*	0.977 (0.872, 0.997)*	0.982 (0.895, 0.997)*	0.979 (0.878, 0.997)*	0.992 (0.952, 0.999)*
	SNB	0.989 (0.934, 0.998)*	0.965 (0.809, 0.995)*	0.938 (0.677, 0.991)*	0.967 (0.817, 0.995)*	0.971 (0.836, 0.996)*	0.995 (0.970, 0.999)*
	SNGoGn	0.984 (0.908, 0.998)*	0.995 (0.972, 0.999)*	0.983 (0.902, 0.998)*	0.990 (0.944, 0.999)*	0.993 (0.962, 0.999)*	0.998 (0.988, 1.000)*
	L	0.994 (0.953, 0.999)*	0.996 (0.968, 1.000)*	0.995 (0.964, 0.999)*	0.994 (0.958, 0.999)*	0.997 (0.975, 1.000)*	0.999 (0.989, 1.000)*
	Co-A	0.987 (0.953, 0.999)*	0.985 (0.915, 0.998)*	0.985 (0.911, 0.998)*	0.989 (0.933, 0.998)*	0.985 (0.915, 0.998)*	0.996 (0.976, 0.999)*
	Co-Gn	0.994 (0.966, 0.999)*	0.998 (0.991, 1.000)*	0.995 (0.972, 0.999)*	0.997 (0.983, 1.000)*	0.996 (0.975, 0.999)*	0.998 (0.990, 1.000)*
Airway analysis	TOH	0.992 (0.940, 0.999)*	0.997 (0.981, 1.000)*	0.995 (0.961, 0.999)*	0.993 (0.951, 0.999)*	0.997 (0.978, 1.000)*	0.998 (0.987, 1.000)*
	IAV	0.999 (0.999, 1.000)*	0.999 (0.999, 1.000)*	0.999 (0.999, 1.000)*	0.999 (0.999, 1.000)*	0.999 (0.999, 1.000)*	0.999 (0.999, 1.000)*
	NAV	0.999 (0.999, 1.000)*	0.999 (0.999, 1.000)*	0.999 (0.999, 1.000)*	0.999 (0.999, 1.000)*	0.999 (0.999, 1.000)*	0.999 (0.999, 1.000)*
	OAV	0.999 (0.999, 1.000)*	0.999 (0.999, 1.000)*	0.999 (0.999, 1.000)*	0.999 (0.999, 1.000)*	0.999 (0.999, 1.000)*	0.999 (0.999, 1.000)*
	HAV	0.999 (0.998, 1.000)*	0.999 (0.999, 1.000)*	0.999 (0.999, 1.000)*	0.999 (0.999, 1.000)*	0.999 (0.999, 1.000)*	0.999 (0.999, 1.000)*
	MCA	0.999 (0.997, 1.000)*	0.998 (0.982, 1.000)*	0.999 (0.995, 1.000)*	0.996 (0.972, 1.000)*	0.998 (0.987, 1.000)*	0.999 (0.998, 1.000)*

\* Statistical significance of the ICC value.

<sup>a</sup>ANFW indicates anterior nasal floor width; ANW, anterior nasal width; CI, confidence interval; Co-A, Condylion to point A; Co-Gn, Condylion to Gnathion; EMW, external maxillary width; FMR-l, frontomaxillary suture right to left; FZR-l, frontozygomatic right to left; HAV, hypopharyngeal airway volume; IAV, intraoral airway volume; ICC, intraclass correlation coefficients; INCr-l, inner nasal contour point right to left; Inter-Mcf, intermolar width at the first molar central fossa level; Inter-Mpa, intermolar width at the first molar palatal apex level; L, lordosis angle; MCA, minimum cross-sectional area in oropharynx; MDCT, multidetector computed tomography; NAV, nasopharyngeal airway volume; OAV, oropharyngeal airway volume; PNFW, posterior nasal floor width; PNW, posterior nasal width; PW, palatal width; SNA, Sella-Nasion-subspinal angle; SNB, Sella-Nasion-supramentale angle; SNGoGn, Sella-Nasion-Gonion-Gnathion angle; TOH, total oropharynx height; ZMLr-l, zygomaticomaxillary lower right to left; ZMUR-l, zygomaticomaxillary upper right to left; ZTUR-l, zygomaticotemporal suture upper right to left.

chart is detailed in Figure 1. Additionally, a dry skull underwent both CBCT and MDCT scans (SKULL group) as the gold standard. All images were reconstructed and exported as digital imaging and communications in medicine (DICOM) files.

### Duplication and Randomization of the DICOM Files

The corresponding author duplicated the MDCT and CBCT DICOM files (five subjects and one dry skull), created 24 files, and randomly assigned code numbers to each. Six orthodontic residents imported these files into two software programs: Dolphin Imaging Version 11.9 Premium (Dolphin Imaging and Management Solutions, Chatsworth, CA) and Amira software (version 2022.1, Thermo Fischer Scientific, Merignac, France), unaware that the data were duplicates. They believed the data represented 20 individuals/subjects

and four dry skulls, not knowing that they were being evaluated for intra-examiner reliability. Before the study, the examiners were trained on importing DICOM files, orienting images, and measuring the 26 variables, and were given a step-by-step illustrated handout.

### Image Processing and Dimensional Measurements

After importing the CT data into Dolphin or Amira, examiners reoriented head positions. Before measurements, HU calibration/correction was conducted using Amira but not Dolphin, as Dolphin lacked this function.

The study involved 26 common airway-related measurements categorized into eight linear orthogonal,<sup>15–17</sup> six linear 3D surface rendering,<sup>18–20</sup> six lateral cephalometric,<sup>21</sup> and six airway analysis parameters.<sup>22,23</sup> Table 1 outlines the definition of each measurement. Semi-automatic segmentation was used for airway

**Table 3.** Intra-Examiner Reliabilities Estimated by Intraclass Correlation Coefficients (ICCs) for Repeated Measurements on Cone-Beam Computed Tomography (CBCT) Images Using Amira

CBCT × Amira	Variable	Examiner A ICC (95% CI)	Examiner B ICC (95% CI)	Examiner C ICC (95% CI)	Examiner D ICC (95% CI)	Examiner E ICC (95% CI)	Examiner F ICC (95% CI)
Linear measurements on the orthogonal planes	ANW	0.979 (0.855, 0.998)*	0.979 (0.855, 0.998)*	0.961 (0.742, 0.996)*	0.931 (0.580, 0.992)*	0.923 (0.545, 0.992)*	0.983 (0.884, 0.998)*
	ANFW	0.987 (0.906, 0.999)*	0.987 (0.906, 0.999)*	0.972 (0.813, 0.997)*	0.987 (0.909, 0.999)*	0.928 (0.568, 0.992)*	0.989 (0.924, 0.999)*
	PNW	0.797 (0.386, 0.954)*	0.795 (0.324, 0.936)*	0.914 (0.500, 0.990)*	0.962 (0.748, 0.996)*	0.955 (0.710, 0.995)*	0.993 (0.946, 0.999)*
	PNFW	0.969 (0.794, 0.997)*	0.969 (0.794, 0.997)*	0.968 (0.786, 0.997)*	0.978 (0.849, 0.998)*	0.980 (0.861, 0.998)*	0.997 (0.980, 1.000)*
	EMW	0.987 (0.911, 0.999)*	0.987 (0.911, 0.999)*	0.996 (0.970, 1.000)*	0.996 (0.972, 1.000)*	0.966 (0.773, 0.996)*	0.996 (0.972, 1.000)*
	PW	0.968 (0.822, 0.995)*	0.968 (0.822, 0.995)*	0.949 (0.731, 0.993)*	0.962 (0.792, 0.994)*	0.935 (0.664, 0.990)*	0.995 (0.971, 0.999)*
	Inter-Mpa	0.980 (0.887, 0.997)*	0.980 (0.887, 0.997)*	0.989 (0.937, 0.998)*	0.990 (0.944, 0.999)*	0.978 (0.874, 0.997)*	0.996 (0.974, 0.999)*
Linear measurements on the three-dimensional (3D) surface rendering images	Inter-Mcf	0.991 (0.933, 0.999)*	0.991 (0.933, 0.999)*	0.983 (0.878, 0.998)*	0.991 (0.935, 0.999)*	0.985 (0.892, 0.998)*	0.995 (0.964, 0.999)*
	ZTUR-l	0.994 (0.965, 0.999)*	0.994 (0.965, 0.999)*	0.996 (0.975, 0.999)*	0.996 (0.979, 0.999)*	0.997 (0.970, 1.000)*	0.999 (0.999, 1.000)*
	FMr-l	0.958 (0.729, 0.995)*	0.958 (0.729, 0.995)*	0.937 (0.613, 0.993)*	0.934 (0.596, 0.993)*	0.924 (0.549, 0.992)*	0.993 (0.946, 0.999)*
	FZr-l	0.981 (0.890, 0.997)*	0.981 (0.890, 0.997)*	0.995 (0.969, 0.999)*	0.996 (0.974, 0.999)*	0.993 (0.957, 0.999)*	0.999 (0.996, 1.000)*
	INCr-l	0.951 (0.737, 0.993)*	0.951 (0.737, 0.993)*	0.928 (0.636, 0.989)*	0.950 (0.736, 0.993)*	0.938 (0.678, 0.991)*	0.990 (0.939, 0.998)*
	ZMUr-l	0.995 (0.953, 1.000)*	0.995 (0.953, 1.000)*	0.991 (0.917, 0.999)*	0.970 (0.736, 0.998)*	0.986 (0.867, 0.999)*	0.999 (0.991, 1.000)*
	ZMLr-l	0.975 (0.829, 0.997)*	0.975 (0.829, 0.997)*	0.959 (0.734, 0.996)*	0.979 (0.853, 0.998)*	0.978 (0.848, 0.998)*	0.965 (0.770, 0.996)*
Lateral cephalometric analysis	SNA	0.980 (0.887, 0.997)*	0.980 (0.887, 0.997)*	0.988 (0.928, 0.998)*	0.984 (0.911, 0.998)*	0.980 (0.888, 0.997)*	0.997 (0.983, 1.000)*
	SNB	0.966 (0.812, 0.995)*	0.966 (0.812, 0.995)*	0.959 (0.780, 0.994)*	0.976 (0.866, 0.997)*	0.976 (0.862, 0.996)*	0.997 (0.983, 1.000)*
	SNGoGn	0.979 (0.878, 0.997)*	0.979 (0.878, 0.997)*	0.986 (0.920, 0.998)*	0.992 (0.954, 0.999)*	0.994 (0.964, 0.999)*	0.998 (0.989, 1.000)*
	L	0.998 (0.982, 1.000)*	0.998 (0.982, 1.000)*	0.997 (0.979, 1.000)*	0.996 (0.969, 1.000)*	0.998 (0.982, 1.000)*	0.999 (0.996, 1.000)*
	Co-A	0.982 (0.896, 0.997)*	0.982 (0.896, 0.997)*	0.977 (0.868, 0.997)*	0.981 (0.890, 0.997)*	0.974 (0.853, 0.996)*	0.998 (0.985, 1.000)*
	Co-Gn	0.994 (0.962, 0.999)*	0.994 (0.962, 0.999)*	0.996 (0.979, 0.999)*	0.936 (0.668, 0.991)*	0.994 (0.964, 0.999)*	0.999 (0.994, 1.000)*
	TOH	0.996 (0.973, 1.000)*	0.996 (0.973, 1.000)*	0.994 (0.956, 0.999)*	0.997 (0.977, 1.000)*	0.996 (0.970, 1.000)*	0.998 (0.986, 1.000)*
Airway analysis	IAV	0.999 (0.999, 1.000)*	0.999 (0.999, 1.000)*	0.999 (0.999, 1.000)*	0.999 (0.999, 1.000)*	0.999 (0.999, 1.000)*	0.999 (0.999, 1.000)*
	NAV	0.999 (0.998, 1.000)*	0.999 (0.998, 1.000)*	0.999 (0.999, 1.000)*	0.999 (0.998, 1.000)*	0.999 (0.997, 1.000)*	0.999 (0.999, 1.000)*
	OAV	0.999 (0.999, 1.000)*	0.999 (0.999, 1.000)*	0.999 (0.999, 1.000)*	0.999 (0.999, 1.000)*	0.999 (0.999, 1.000)*	0.999 (0.999, 1.000)*
	HAV	0.999 (0.996, 1.000)*	0.999 (0.996, 1.000)*	0.999 (0.995, 1.000)*	0.999 (0.999, 1.000)*	0.999 (0.995, 1.000)*	0.999 (0.999, 1.000)*
	MCA	0.997 (0.977, 1.000)*	0.997 (0.977, 1.000)*	0.998 (0.987, 1.000)*	0.993 (0.952, 0.999)*	0.994 (0.953, 0.999)*	0.998 (0.987, 1.000)*

\*Statistical significance of the ICC value.

<sup>a</sup> ANFW indicates anterior nasal floor width; ANW, anterior nasal width; CBCT: cone-beam computed tomography; CI, confidence interval; Co-A, Condylion to point A; Co-Gn, Condylion to Gnathion; EMW, external maxillary width; FMr-l, frontomaxillary suture right to left; FZr-l, frontozygomatic right to left; HAV, hypopharyngeal airway volume; IAV, intraoral airway volume; ICC, intraclass correlation coefficients; INCr-l, inner nasal contour point right to left; Inter-Mcf, intermolar width at the first molar central fossa level; Inter-Mpa, intermolar width at the first molar palatal apex level; L, lordosis angle; MCA, minimum cross-sectional area in oropharynx; NAV, nasopharyngeal airway volume; OAV, oropharyngeal airway volume; PNFW, posterior nasal floor width; PNW, posterior nasal width; PW, palatal width; SNA, Sella-Nasion-subspinale angle; SNB, Sella-Nasion-supramentale angle; SNGoGn, Sella-Nasion-Gonion-Gnathion angle; TOH, total oropharynx height; ZMLr-l, zygomaticomaxillary lower right to left; ZMUr-l, zygomaticomaxillary upper right to left; ZTUR-l, zygomaticotemporal suture upper right to left.

measurements, with manual selection of boundaries and threshold sensitivity setting. Airway parameters or spinal curvature were not measured in the SKULL group due to absence of soft tissue and the cervical spine in the dry skull.

### Statistical Analysis

Raw data were entered into an Excel file, and R statistical software (version 4.2.3; <https://www.r-project.org>) was used for scatterplots and statistical calculations. Intra- and inter-examiner reliability were determined using the intraclass correlation coefficient (ICC)<sup>24</sup> with 95% confidence intervals (95% CIs). Reliability grades ranged from poor (ICC: 0.00 ~ 0.10), slight (ICC: 0.11 ~ 0.20), fair (ICC: 0.21 ~ 0.40), moderate (ICC: 0.41 ~ 0.60), substantial (ICC: 0.61 ~ 0.80), almost perfect (ICC: 0.81 ~ 0.99), and perfect agreement (ICC: 1.00).

Regression analysis created prediction models for each variable, considering imaging modality (MDCT or CBCT), measurement software (Amira or Dolphin), subject type (skull or patient), and specific examiner (1 to 6). The model was expressed mathematically as:

$$Y_i = \mu + \tau_1 D_1 + \tau_2 D_2 + \tau_3 D_3 + \alpha_i + \tau_1 D_1 \times \tau_2 D_2 + \tau_1 D_1 \times \tau_3 D_3 + \tau_2 D_2 \times \tau_3 D_3 + \varepsilon_i$$

$Y_i$  was the measured value from number- $i$  examiner;  $\mu$  the average value from all examiners;  $\tau_1 D_1$  the dummy variable for imaging modality ( $D_1 = 1$  for MDCT;  $D_1 = 0$  for CBCT);  $\tau_2 D_2$  the dummy variable for software ( $D_2 = 1$  for Amira;  $D_2 = 0$  for Dolphin);  $\tau_3 D_3$  the dummy variable for subject ( $D_3 = 1$  for skull;  $D_3 = 0$  for patient);  $\alpha_i$  the fixed effect of the number- $i$  examiner;  $\tau_1 D_1 \times \tau_2 D_2$  the interaction effect

**Table 4.** Intra-Examiner Reliabilities Estimated by Intra-Class Correlation Coefficients (ICCs) for Repeated Measurements on Multidetector Computed Tomography (MDCT) Images Using Dolphin

MDCT × Dolphin	Variable	Examiner A ICC (95% CI)	Examiner B ICC (95% CI)	Examiner C ICC (95% CI)	Examiner D ICC (95% CI)	Examiner E ICC (95% CI)	Examiner F ICC (95% CI)
Linear measurements on the orthogonal planes	ANW	0.915 (0.504, 0.991)*	0.624 (0.495, 0.935)*	0.785 (0.059, 0.975)*	0.869 (0.316, 0.985)*	0.870 (0.323, 0.985)*	0.911 (0.489, 0.990)*
	ANFW	0.914 (0.503, 0.990)*	0.942 (0.636, 0.994)*	0.926 (0.557, 0.992)*	0.855 (0.268, 0.983)*	0.919 (0.526, 0.991)*	0.855 (0.267, 0.983)*
	PNW	0.761 (0.302, 0.957)*	0.791 (0.074, 0.975)*	0.848 (0.245, 0.983)*	0.758 (0.409, 0.971)*	0.958 (0.728, 0.995)*	0.827 (0.478, 0.980)*
	PNFW	0.950 (0.680, 0.995)*	0.911 (0.489, 0.990)*	0.974 (0.822, 0.997)*	0.923 (0.544, 0.992)*	0.876 (0.345, 0.986)*	0.929 (0.573, 0.992)*
	EMW	0.988 (0.914, 0.999)*	0.975 (0.832, 0.997)*	0.953 (0.697, 0.995)*	0.982 (0.874, 0.998)*	0.967 (0.779, 0.996)*	0.954 (0.701, 0.995)*
	PW	0.910 (0.559, 0.987)*	0.887 (0.471, 0.983)*	0.955 (0.759, 0.993)*	0.926 (0.628, 0.989)*	0.927 (0.628, 0.989)*	0.821 (0.259, 0.972)*
	Inter-Mpa	0.969 (0.828, 0.996)*	0.878 (0.440, 0.982)*	0.963 (0.798, 0.995)*	0.952 (0.743, 0.993)*	0.956 (0.762, 0.994)*	0.968 (0.821, 0.995)*
	Inter-Mcf	0.989 (0.923, 0.999)*	0.995 (0.966, 1.000)*	0.983 (0.882, 0.998)*	0.984 (0.887, 0.998)*	0.980 (0.863, 0.998)*	0.989 (0.924, 0.999)*
Linear measurements on the three-dimensional (3D) surface rendering images	ZTUR-l	0.997 (0.982, 1.000)*	0.990 (0.942, 0.999)*	0.992 (0.955, 0.999)*	0.997 (0.984, 1.000)*	0.997 (0.981, 1.000)*	0.994 (0.963, 0.999)*
	FMr-l	0.751 (0.525, 0.970)*	0.900 (0.442, 0.989)*	0.821 (0.158, 0.979)*	0.923 (0.545, 0.992)*	0.935 (0.602, 0.993)*	0.921 (0.532, 0.991)*
	FZr-l	0.972 (0.845, 0.996)*	0.996 (0.974, 0.999)*	0.984 (0.905, 0.998)*	0.978 (0.874, 0.997)*	0.987 (0.924, 0.998)*	0.991 (0.947, 0.999)*
	INCr-l	0.934 (0.661, 0.990)*	0.830 (0.285, 0.974)*	0.842 (0.322, 0.976)*	0.943 (0.699, 0.992)*	0.960 (0.785, 0.994)*	0.946 (0.714, 0.992)*
	ZMUr-l	0.934 (0.493, 0.996)*	0.986 (0.869, 0.999)*	0.986 (0.873, 0.999)*	0.991 (0.910, 0.999)*	0.996 (0.959, 1.000)*	0.982 (0.836, 0.999)*
	ZMLr-l	0.930 (0.579, 0.992)*	0.978 (0.848, 0.998)*	0.962 (0.751, 0.996)*	0.956 (0.712, 0.995)*	0.989 (0.922, 0.999)*	0.892 (0.405, 0.988)*
Lateral cephalometric analysis	SNA	0.972 (0.843, 0.996)*	0.960 (0.783, 0.994)*	0.979 (0.881, 0.997)*	0.976 (0.865, 0.997)*	0.953 (0.747, 0.993)*	0.993 (0.962, 0.999)*
	SNB	0.984 (0.910, 0.998)*	0.944 (0.708, 0.992)*	0.965 (0.809, 0.995)*	0.985 (0.912, 0.998)*	0.967 (0.818, 0.995)*	0.996 (0.977, 0.999)*
	SNGoGn	0.963 (0.798, 0.995)*	0.970 (0.833, 0.996)*	0.986 (0.920, 0.998)*	0.960 (0.785, 0.994)*	0.984 (0.906, 0.998)*	0.973 (0.847, 0.996)*
	L	0.975 (0.831, 0.997)*	0.976 (0.834, 0.997)*	0.985 (0.893, 0.998)*	0.994 (0.958, 0.999)*	0.988 (0.917, 0.999)*	0.983 (0.881, 0.998)*
	Co-A	0.907 (0.549, 0.986)*	0.975 (0.858, 0.996)*	0.939 (0.681, 0.991)*	0.970 (0.834, 0.996)*	0.974 (0.852, 0.996)*	0.979 (0.881, 0.997)*
	Co-Gn	0.990 (0.940, 0.999)*	0.990 (0.941, 0.999)*	0.990 (0.942, 0.999)*	0.997 (0.983, 1.000)*	0.996 (0.979, 0.999)*	0.996 (0.974, 0.999)*
Airway analysis	TOH	0.979 (0.853, 0.998)*	0.978 (0.850, 0.998)*	0.976 (0.881, 0.997)*	0.981 (0.870, 0.998)*	0.994 (0.954, 0.999)*	0.965 (0.769, 0.996)*
	IAV	0.985 (0.860, 0.999)*	0.993 (0.934, 1.000)*	0.997 (0.970, 1.000)*	0.995 (0.953, 1.000)*	0.999 (0.995, 1.000)*	0.968 (0.724, 0.998)*
	NAV	0.994 (0.958, 0.999)*	0.989 (0.923, 0.999)*	0.993 (0.951, 0.999)*	0.989 (0.920, 0.999)*	0.987 (0.908, 0.999)*	0.942 (0.639, 0.994)*
	OAV	0.971 (0.802, 0.997)*	0.984 (0.885, 0.998)*	0.999 (0.991, 1.000)*	0.986 (0.899, 0.998)*	0.984 (0.890, 0.998)*	0.943 (0.643, 0.994)*
	HAV	0.850 (0.451, 0.983)*	0.977 (0.841, 0.998)*	0.997 (0.977, 1.000)*	0.984 (0.886, 0.998)*	0.987 (0.904, 0.999)*	0.869 (0.319, 0.985)*
	MCA	0.864 (0.299, 0.985)*	0.958 (0.727, 0.995)*	0.897 (0.426, 0.988)*	0.725 (0.360, 0.952)*	0.784 (0.355, 0.974)*	0.701 (0.301, 0.869)*

\* Statistical significance of the ICC value.

<sup>a</sup>ANFW indicates anterior nasal floor width; ANW, anterior nasal width; CI, confidence interval; Co-A, Condylion to point A; Co-Gn, Condylion to Gnathion; EMW, external maxillary width; FMr-l, frontomaxillary suture right to left; FZr-l, frontozygomatic right to left; HAV, hypopharyngeal airway volume; IAV, intraoral airway volume; ICC, intraclass correlation coefficients; INCr-l, inner nasal contour point right to left; Inter-Mcf, intermolar width at the first molar central fossa level; Inter-Mpa, intermolar width at the first molar palatal apex level; L, lordosis angle; MCA, minimum cross-sectional area in oropharynx; MDCT, multi-detector computed tomography; NAV, nasopharyngeal airway volume; OAV, oropharyngeal airway volume; PNFW, posterior nasal floor width; PNW, posterior nasal width; PW, palatal width; SNA, Sella-Nasion-subspinale angle; SNB, Sella-Nasion-supramentale angle; SNGoGn: Sella-Nasion-Gonion-Gnathion angle; TOH, total oropharynx height; ZMLr-l, zygomaticomaxillary lower right to left; ZMUr-l, Zygomaticomaxillary upper right to left; ZTUR-l, zygomaticotemporal suture upper right to left.

of imaging modality and software;  $\tau_1 D_1 \times \tau_3 D_3$  the interaction effect of imaging modality and type of subject;  $\tau_2 D_2 \times \tau_3 D_3$  the interaction effect of software and type of subject; and  $\epsilon_i$  the residual error. Measurement agreement was evaluated using Wilcoxon sign rank test, with significance level set at 0.05.

**RESULTS**

Tables 2 through 6 provide detailed ICC values for intra- and inter-examiner reliability.

**Intra-examiner Reliability**

In MDCT × Amira and CBCT × Amira groups, all examiners demonstrated “almost perfect” intra-examiner agreement, except for one MDCT examiner and two CBCT examiners with “substantial” agreement in the variable PNW (Tables 2 and 3). In

MDCTxDolphin group, most examiners had “almost perfect” intra-examiner agreement, except for variables ANW, PNW, FMr-l, and MCA, which showed only “substantial” agreement (Table 4). In CBCT × Dolphin group, most examiners demonstrated “almost perfect” intra-examiner agreement, except for ANW, PNW, and FMr-l. All examiners had “moderate” to “substantial” agreement for ANW (ICC: 0.601–0.770). Three examiners showed “moderate” to “substantial” agreement for PNW and FMr-l (ICCs: 0.628–0.719) (Table 5).

**Inter-observer Reliability**

In MDCT × Amira and CBCT × Amira groups, inter-examiner agreement was “almost perfect” for all measurements, except for PNW, which showed ICCs of 0.769 (MDCT) and 0.793 (CBCT). In MDCTxDolphin group, inter-examiner agreement was “substantial” for ANW, PNW, FMr-l, and MCA, while other measurements

**Table 5.** Intra-Examiner Reliabilities Estimated by Intraclass Correlation Coefficients (ICCs) for Repeated Measurements on Cone-Beam Computed Tomography (CBCT) Images Using Dolphin

CBCT × Dolphin	Variable	Examiner A	Examiner B	Examiner C	Examiner D	Examiner E	Examiner F
		ICC (95% CI)					
Linear measurements on the orthogonal planes	ANW	0.639 (0.275, 0.644)*	0.770 (0.321, 0.985)*	0.608 (0.358, 0.869)*	0.686 (0.218, 0.946)*	0.601 (0.497, 0.892)*	0.624 (0.381, 0.897)*
	ANFW	0.947 (0.668, 0.994)*	0.851 (0.254, 0.983)*	0.920 (0.527, 0.991)*	0.913 (0.498, 0.990)*	0.968 (0.788, 0.997)*	0.956 (0.713, 0.995)*
	PNW	0.875 (0.340, 0.986)*	0.679 (0.445, 0.927)*	0.682 (0.366, 0.960)*	0.665 (0.387, 0.783)*	0.911 (0.489, 0.990)*	0.864 (0.300, 0.985)*
	PNFW	0.990 (0.928, 0.999)*	0.831 (0.191, 0.981)*	0.974 (0.821, 0.997)*	0.903 (0.454, 0.989)*	0.842 (0.223, 0.982)*	0.986 (0.901, 0.998)*
	EMW	0.989 (0.919, 0.999)*	0.952 (0.690, 0.995)*	0.978 (0.851, 0.998)*	0.976 (0.838, 0.997)*	0.974 (0.822, 0.997)*	0.993 (0.946, 0.999)*
	PW	0.913 (0.571, 0.987)*	0.903 (0.534, 0.986)*	0.913 (0.573, 0.987)*	0.931 (0.647, 0.990)*	0.898 (0.512, 0.985)*	0.876 (0.431, 0.981)*
	Inter-Mpa	0.983 (0.900, 0.997)*	0.948 (0.724, 0.992)*	0.978 (0.878, 0.997)*	0.957 (0.768, 0.994)*	0.959 (0.775, 0.994)*	0.989 (0.937, 0.998)*
	Inter-Mcf	0.986 (0.899, 0.998)*	0.992 (0.941, 0.999)*	0.976 (0.837, 0.997)*	0.976 (0.838, 0.997)*	0.986 (0.900, 0.998)*	0.995 (0.965, 0.999)*
Linear measurements on the three-dimensional (3D) surface rendering images	ZTUR-l	0.984 (0.905, 0.998)*	0.989 (0.937, 0.998)*	0.993 (0.961, 0.999)*	0.992 (0.953, 0.999)*	0.995 (0.972, 0.999)*	0.995 (0.971, 0.999)*
	FMr-l	0.628 (0.256, 0.952)*	0.921 (0.533, 0.991)*	0.828 (0.179, 0.980)*	0.682 (0.342, 0.928)*	0.719 (0.401, 0.935)*	0.851 (0.254, 0.983)*
	FZr-l	0.984 (0.906, 0.998)*	0.981 (0.892, 0.997)*	0.987 (0.923, 0.998)*	0.987 (0.926, 0.998)*	0.987 (0.926, 0.998)*	0.988 (0.931, 0.998)*
	INCr-l	0.906 (0.543, 0.986)*	0.803 (0.210, 0.969)*	0.801 (0.204, 0.969)*	0.851 (0.350, 0.977)*	0.918 (0.592, 0.988)*	0.910 (0.560, 0.987)*
	ZMUr-l	0.955 (0.629, 0.997)*	0.926 (0.443, 0.995)*	0.945 (0.560, 0.996)*	0.985 (0.857, 0.999)*	0.980 (0.819, 0.999)*	0.901 (0.314, 0.993)*
	ZMLr-l	0.916 (0.512, 0.991)*	0.860 (0.286, 0.984)*	0.944 (0.648, 0.994)*	0.941 (0.633, 0.994)*	0.975 (0.826, 0.997)*	0.923 (0.543, 0.991)*
Lateral cephalometric analysis	SNA	0.983 (0.904, 0.998)*	0.966 (0.814, 0.995)*	0.984 (0.907, 0.998)*	0.991 (0.946, 0.999)*	0.979 (0.879, 0.997)*	0.983 (0.904, 0.998)*
	SNB	0.991 (0.946, 0.999)*	0.973 (0.847, 0.996)*	0.875 (0.429, 0.981)*	0.985 (0.913, 0.998)*	0.963 (0.797, 0.995)*	0.985 (0.912, 0.998)*
	SNGoGn	0.961 (0.786, 0.994)*	0.974 (0.853, 0.996)*	0.975 (0.858, 0.996)*	0.987 (0.926, 0.998)*	0.991 (0.948, 0.999)*	0.977 (0.869, 0.997)*
	L	0.993 (0.953, 0.999)*	0.990 (0.928, 0.999)*	0.993 (0.946, 0.999)*	0.993 (0.950, 0.999)*	0.997 (0.982, 1.000)*	0.991 (0.934, 0.999)*
	Co-A	0.979 (0.882, 0.997)*	0.954 (0.755, 0.993)*	0.977 (0.870, 0.997)*	0.979 (0.880, 0.997)*	0.986 (0.920, 0.998)*	0.985 (0.916, 0.998)*
	Co-Gn	0.982 (0.897, 0.997)*	0.985 (0.911, 0.998)*	0.990 (0.943, 0.999)*	0.995 (0.969, 0.999)*	0.993 (0.960, 0.999)*	0.995 (0.969, 0.999)*
Airway analysis	TOH	0.991 (0.932, 0.999)*	0.984 (0.889, 0.998)*	0.987 (0.908, 0.999)*	0.985 (0.895, 0.998)*	0.996 (0.968, 1.000)*	0.990 (0.930, 0.999)*
	IaV	0.905 (0.410, 0.997)*	0.971 (0.619, 0.999)*	0.930 (0.266, 0.998)*	0.994 (0.905, 1.000)*	0.985 (0.790, 1.000)*	0.915 (0.469, 0.998)*
	NaV	0.929 (0.570, 0.992)*	0.994 (0.959, 0.999)*	0.996 (0.973, 1.000)*	0.986 (0.900, 0.998)*	0.969 (0.790, 0.997)*	0.940 (0.630, 0.993)*
	OaV	0.987 (0.911, 0.999)*	0.983 (0.882, 0.998)*	0.986 (0.904, 0.999)*	0.990 (0.926, 0.999)*	0.998 (0.987, 1.000)*	0.981 (0.867, 0.998)*
	HaV	0.945 (0.380, 0.999)*	0.975 (0.658, 0.999)*	0.976 (0.679, 0.999)*	0.983 (0.754, 1.000)*	0.996 (0.942, 1.000)*	0.879 (0.355, 0.986)*
	MCA	0.986 (0.901, 0.999)*	0.940 (0.627, 0.993)*	0.963 (0.755, 0.996)*	0.991 (0.932, 0.999)*	0.937 (0.612, 0.993)*	0.905 (0.408, 0.997)*

\*Statistical significance of the ICC value.

<sup>a</sup> ANFW indicates anterior nasal floor width; ANW, anterior nasal width; CBCT, cone-beam computed tomography; CI, confidence interval; Co-A, Condylion to point A; Co-Gn, Condylion to Gnathion; EMW, external maxillary width; FMr-l, frontomaxillary suture right to left; FZr-l, frontozygomatic right to left; HAV, hypopharyngeal airway volume; IAV, intraoral airway volume; ICC, intraclass correlation coefficients; INCr-l, inner nasal contour point right to left; Inter-Mcf, intermolar width at the first molar central fossa level; Inter-Mpa, intermolar width at the first molar palatal apex level; L, lordosis angle; MCA, minimum cross-sectional area in oropharynx; NAV, nasopharyngeal airway volume; OAV, oropharyngeal airway volume; PNFW, posterior nasal floor width; PNW, posterior nasal width; PW, palatal width; SNA, Sella-Nasion-subspinale angle; SNB, Sella-Nasion-supramentale angle; SNGoGn: Sella-Nasion-Gonion-Gnathion angle; TOH, total oropharynx height; ZMLr-l, zygomaticomaxillary lower right to left; ZMUr-l, zygomaticomaxillary upper right to left; ZTUR-l, zygomaticotemporal suture upper right to left.

indicated “almost perfect” agreement. In CBCTxDolphin group, interexaminer agreement was “substantial” for ANW, PNW, FMr-l, and INCr-l, while other measurements indicated “almost perfect” agreement (Table 6).

### Comparison of the Measurements Acquired using Amira and Dolphin

Average measurements using Amira and Dolphin on the same CT scans by all examiners are presented in Tables 7 through 9. Significant differences in most variables were observed between the two software programs regardless of the imaging modality (MDCT or CBCT). Volumetric airway measurements showed larger standard deviations with Dolphin, often 10 to 30 times more (Tables 7 and 8). Approximately half of the variables in the SKULL group exhibited significant differences between Amira and Dolphin measurements (Table 9). In the

SKULL group, all standard deviations were within one unit (1 mm or degree). For patient images, Dolphin had standard deviations exceeding one unit for all linear and angular variables, while Amira exceeded one unit only for PNW, ZTUR-l, ZMU r-l, ZML r-l, L, and Go-Gn.

### Regression Model for each Variable

Tables 10 through 13 summarize how variables were affected by imaging modalities (MDCT or CBCT), measurement software (Amira or Dolphin), subject type (skull or patient), and specific examiner. Significant factors ( $P < 0.05$ ) are explained by their estimate values. Imaging modalities significantly influenced ANFW, FMr-l, INCr-l, ZMLr-l, SNGoGn, NAV, OAV, HAV, and MCA. Software affected ANW, PNW, PNFW, FMr-l, NAV, OAV, HAV, and MCA. Subject type impacted ANW, ANFW, PNW, PNFW, EMW, PW, ZTUR-l, FMr-l,

**Table 6.** Interexaminer Reliabilities Estimated by Intraclass Correlation Coefficients (ICCs) For Each Measurement

Category	Imaging Modality Software Variable	MDCT		CBCT	
		Amira		Dolphin	
		ICC (95% CI)	ICC (95% CI)	ICC (95% CI)	ICC (95% CI)
Linear measurements on the orthogonal planes	ANW	0.892 (0.769, 0.967)*	0.912 (0.809, 0.973)*	0.761 (0.552, 0.92)*	0.653 (0.398, 0.818)*
	ANFW	0.964 (0.918, 0.989)*	0.959 (0.906, 0.988)*	0.869 (0.725, 0.959)*	0.895 (0.778, 0.968)*
	PNW	0.769 (0.554, 0.924)*	0.793 (0.602, 0.932)*	0.669 (0.429, 0.881)*	0.630 (0.384, 0.863)*
	PNFW	0.952 (0.892, 0.986)*	0.965 (0.920, 0.990)*	0.850 (0.696, 0.953)*	0.895 (0.775, 0.968)*
	EMW	0.983 (0.959, 0.995)*	0.978 (0.948, 0.993)*	0.972 (0.936, 0.992)*	0.961 (0.909, 0.989)*
	PW	0.954 (0.903, 0.984)*	0.917 (0.829, 0.971)*	0.908 (0.804, 0.968)*	0.914 (0.825, 0.970)*
	Inter-Mpa	0.956 (0.906, 0.985)*	0.970 (0.935, 0.990)*	0.941 (0.873, 0.980)*	0.934 (0.863, 0.977)*
	Inter-Mcf	0.977 (0.946, 0.993)*	0.981 (0.956, 0.995)*	0.974 (0.940, 0.993)*	0.834 (0.669, 0.947)*
Linear measurements on the three-dimensional (3D) surface rendering images	ZTUr-l	0.996 (0.992, 0.999)*	0.994 (0.987, 0.998)*	0.993 (0.984, 0.998)*	0.992 (0.982, 0.997)*
	FMr-l	0.908 (0.802, 0.972)*	0.920 (0.825, 0.976)*	0.779 (0.581, 0.927)*	0.715 (0.463, 0.857)*
	FZr-l	0.988 (0.974, 0.996)*	0.991 (0.981, 0.997)*	0.980 (0.957, 0.993)*	0.973 (0.942, 0.991)*
	INCr-l	0.890 (0.774, 0.962)*	0.849 (0.709, 0.945)*	0.830 (0.678, 0.937)*	0.706 (0.497, 0.883)*
	ZMUr-l	0.983 (0.956, 0.996)*	0.982 (0.955, 0.996)*	0.957 (0.893, 0.990)*	0.960 (0.899, 0.990)*
Lateral cephalometric analysis	ZMLr-l	0.983 (0.960, 0.995)*	0.960 (0.910, 0.988)*	0.965 (0.920, 0.990)*	0.929 (0.843, 0.979)*
	SNA	0.978 (0.953, 0.993)*	0.985 (0.967, 0.995)*	0.931 (0.857, 0.976)*	0.973 (0.942, 0.991)*
	SNB	0.966 (0.927, 0.988)*	0.975 (0.946, 0.992)*	0.954 (0.902, 0.984)*	0.954 (0.902, 0.984)*
	SNGoGn	0.988 (0.974, 0.996)*	0.984 (0.964, 0.995)*	0.958 (0.911, 0.986)*	0.983 (0.962, 0.994)*
	L	0.992 (0.980, 0.998)*	0.996 (0.991, 0.999)*	0.981 (0.955, 0.994)*	0.993 (0.984, 0.998)*
	Co-A	0.983 (0.962, 0.994)*	0.981 (0.958, 0.994)*	0.956 (0.905, 0.985)*	0.964 (0.922, 0.988)*
	Co-Gn	0.995 (0.989, 0.998)*	0.980 (0.956, 0.993)*	0.989 (0.976, 0.996)*	0.988 (0.974, 0.996)*
	TOH	0.990 (0.977, 0.997)*	0.992 (0.981, 0.998)*	0.971 (0.932, 0.991)*	0.975 (0.941, 0.993)*
Airway analysis	IAV	0.999 (0.999, 1.000)*	0.999 (0.999, 1.000)*	0.989 (0.972, 0.997)*	0.943 (0.842, 0.990)*
	NAV	0.999 (0.999, 1.000)*	0.999 (0.999, 1.000)*	0.978 (0.949, 0.994)*	0.965 (0.919, 0.990)*
	OAV	0.999 (0.999, 1.000)*	0.999 (0.999, 1.000)*	0.975 (0.943, 0.993)*	0.987 (0.970, 0.996)*
	HAV	0.999 (0.999, 1.000)*	0.999 (0.999, 1.000)*	0.951 (0.889, 0.985)*	0.948 (0.854, 0.991)*
	MCA	0.998 (0.994, 0.999)*	0.994 (0.986, 0.998)*	0.792 (0.557, 0.892)*	0.954 (0.897, 0.986)*

\* Statistical significance of the ICC value.

<sup>a</sup> ANFW indicates anterior nasal floor width; ANW, anterior nasal width; CBCT, cone-beam computed tomography; CI, confidence interval; Co-A, Condylion to point A; Co-Gn, Condylion to Gnathion; EMW, external maxillary width; FMr-l, frontomaxillary suture right to left; FZr-l, frontozygomatic right to left; HAV, hypopharyngeal airway volume; IAV, intraoral airway volume; ICC, intraclass correlation coefficients; INCr-l, inner nasal contour point right to left; Inter-Mcf, intermolar width at the first molar central fossa level; Inter-Mpa, intermolar width at the first molar palatal apex level; L, lordosis angle; MCA, minimum cross-sectional area in oropharynx; NAV, nasopharyngeal airway volume; OAV, oropharyngeal airway volume; PNFw, posterior nasal floor width; PNW, posterior nasal width; PW, palatal width; SNA, Sella-Nasion-subspinale angle; SNB, Sella-Nasion-supramentale angle; SNGoGn: Sella-Nasion-Gonion-Gnathion angle; TOH, total oropharynx height; ZMLr-l, zygomaticomaxillary lower right to left; ZMUr-l, Zygomaticomaxillary upper right to left; ZTUr-l, zygomaticotemporal suture upper right to left.

FZr-l, INCr-l, ZMUr-l, ZMLr-l, SNA, Co-A, and Co-Gn, indicating that the clinical measurements of these variables deviated from the gold standard of SKULL. Only FMr-l and MCA were influenced by the interaction of imaging modalities and software, while PNFw was influenced by the interaction of software and subject type. Examiner did not affect variable values. All airway volumes and areas were significantly reduced on MDCT scans except for IAV. For example, MCA estimate shows 57.784 (-79.467 + 59.283 - 37.6 = -57.784) mm<sup>2</sup> less when measured with Amira on MDCT images.

**DISCUSSION**

There has been growing interest in CBCT assessment in maxillofacial and otorhinolaryngological specialties, particularly regarding airway morphology and

its relationship with sleep-disordered breathing. Many studies have explored the impact of various treatments on airway dimensions, often reporting statistically significant differences, yet overlooking large standard deviations. This raises concerns about the justification for repeated CBCT exposures for research purposes. Therefore, the current study compared intra- and inter-examiner reliability of MDCT and CBCT using Amira and Dolphin software applications for evaluating craniofacial/airway parameters. This study is unique, being the only one that has compared the reliability of both CT modalities with multiple examiners assessing clinical CT images from patients. Results suggested that the software program may have a more significant influence than the image modality on reliability.

**Table 7.** Average Data Obtained by Amira and Dolphin on Multi-Detector Computed Tomography (MDCT) Images for Each Patient

MDCT	Variable	Patient 1			Patient 2		
		MDCT × Amira Mean ± SD	MDCT × Dolphin Mean ± SD	Wilcoxon signed- rank test P value	MDCT × Amira Mean ± SD	MDCT × Dolphin Mean ± SD	Wilcoxon signed-rank test P value
Linear measurements on the orthogonal planes	ANW	31.64 ± 0.69	32.53 ± 0.79	.012*	NA <sup>a</sup>	NA <sup>a</sup>	NA <sup>a</sup>
	ANFW	21.4 ± 0.82	21.41 ± 0.85	>.9	NA <sup>a</sup>	NA <sup>a</sup>	NA <sup>a</sup>
	PNW	32.93 ± 0.76	34.64 ± 1.04	<.001*	NA <sup>a</sup>	NA <sup>a</sup>	NA <sup>a</sup>
	PNFW	28.06 ± 0.76	27.24 ± 0.92	.046*	NA <sup>a</sup>	NA <sup>a</sup>	NA <sup>a</sup>
	EMW	61.95 ± 0.64	64.27 ± 0.76	<.001*	NA <sup>a</sup>	NA <sup>a</sup>	NA <sup>a</sup>
	PW	33.59 ± 0.56	32.27 ± 0.99	.001*	31.58 ± 0.6	34.53 ± 1.88	<.001*
	Inter-Mpa	37.25 ± 0.81	38.31 ± 1.01	.021*	41.82 ± 0.62	41.09 ± 1.23	.11
	Inter-Mcf	46.65 ± 0.46	47.13 ± 0.72	.082*	NA <sup>a</sup>	NA <sup>a</sup>	NA <sup>a</sup>
Linear measurements on the three-dimen- sional (3D) surface rendering images	ZTUR-l	133.08 ± 0.53	133.81 ± 1.19	.056	137.25 ± 0.75	137.54 ± 0.97	.4
	FMR-l	8.22 ± 0.43	6.68 ± 0.39	<.001*	NA <sup>a</sup>	NA <sup>a</sup>	NA <sup>a</sup>
	FZR-l	103.73 ± 0.69	104.81 ± 1.01	.010*	105.34 ± 0.64	106.31 ± 1.23	.053
	INCr-l	27.64 ± 0.7	26.42 ± 0.64	<.001*	24.93 ± 0.46	27.15 ± 0.84	<.001*
	ZMUR-l	73.62 ± 0.86	72.24 ± 1.45	.010*	NA <sup>a</sup>	NA <sup>a</sup>	NA <sup>a</sup>
	ZMLr-l	87.4 ± 0.9	90.46 ± 1.56	<.001*	NA <sup>a</sup>	NA <sup>a</sup>	NA <sup>a</sup>
Lateral cephalometric analysis	SNA	90.32 ± 0.6	88.72 ± 0.98	<.001*	77.77 ± 0.88	77.85 ± 0.69	>.9
	SNB	85.4 ± 0.71	85.78 ± 0.67	.4	78.24 ± 0.81	78.67 ± 1.01	.3
	SNGoGn	33.58 ± 0.75	34.44 ± 1.43	.15	38.22 ± 0.75	39.34 ± 0.97	.014*
	L	103.78 ± 0.94	104.41 ± 1.15	.3	114.27 ± 0.54	114.59 ± 1.14	.3
	Co-A	97.33 ± 0.89	95.88 ± 1.22	.004*	88.28 ± 0.79	89.18 ± 1.34	.083
	Co-Gn	139.66 ± 0.82	140.26 ± 1.2	.15	134.03 ± 0.77	135.1 ± 1.68	.040*
Airway analysis	TOH	63.95 ± 0.55	61.95 ± 0.83	<.001*	75.14 ± 0.7	73.54 ± 1.08	<.001*
	IAV	15561.42 ± 26.81	15342 ± 942.09	>.9	6465 ± 27.84	4940.67 ± 288.03	<.001*
	NAV	4539.33 ± 24.04	6133.67 ± 535.76	<.001*	4324.17 ± 18.09	3373.08 ± 166.72	<.001*
	OAV	13669.25 ± 33.75	13245.5 ± 1724.52	.8	19887.83 ± 34.1	20513.92 ± 1013.86	.2
	HAV	3840.33 ± 28.32	5255.08 ± 438.42	<.001*	7975.42 ± 16.05	7280.58 ± 495.3	.10
	MCA	86.08 ± 4.54	131.58 ± 9.56	<.001*	147.17 ± 5.87	158.92 ± 16.83	<.001*

\* P value < .05 indicates statistical significance.

<sup>a</sup> Data not available because patient had previous midface reconstruction.

<sup>b</sup> Data not available because the upper border of the zygomaticomaxillary suture of this patient was not obvious.

<sup>c</sup> Data not available because there was no intraoral airway space for this patient.

<sup>d</sup> ANFW indicates anterior nasal floor width; ANW, anterior nasal width; CI, confidence interval; Co-A, Condylion to point A; Co-Gn, Condylion to Gnathion; EMW, external maxillary width; FMR-l, frontomaxillary suture right to left; FZR-l, frontozygomatic right to left; HAV, hypopharyngeal airway volume; IAV, intraoral airway volume; ICC, intraclass correlation coefficients; INCr-l, inner nasal contour point right to left; Inter-Mcf, intermolar width at the first molar central fossa level; Inter-Mpa, intermolar width at the first molar palatal apex level; L, lordosis angle; MCA, minimum cross-sectional area in oropharynx; MDCT, multidetector computed tomography; NAV, nasopharyngeal airway volume; OAV, oropharyngeal airway volume; PNFW, posterior nasal floor width; PNW, posterior nasal width; PW, palatal width; SD, standard deviation; SNA, Sella-Nasion-subspinale angle; SNB, Sella-Nasion-supramentale angle; SNGoGn: Sella-Nasion-Gonion-Gnathion angle; TOH, total oropharynx height; ZMLr-l, zygomaticomaxillary lower right to left; ZMUR-l, Zygomaticomaxillary upper right to left; ZTUR-l, zygomaticotemporal suture upper right to left.

Amira, with powerful 3D visualization and animation functions, is expensive and less user-friendly,<sup>25</sup> while Dolphin, favored by orthodontists, lacks airway segmentation control in 2D slices and has noncompatible threshold interval units.<sup>26</sup> Amira's HU calibration function, absent in Dolphin, may explain why Dolphin's airway volume measurements exhibited significantly larger standard deviations. The findings of this study were consistent with the conclusion of de Water et al. that Dolphin was not accurate or reliable for airway analysis.<sup>27</sup>

Zimmerman et al.<sup>14</sup> systematically reviewed 42 studies to assess the reliability of CBCT for upper airway evaluation. Notably, previous studies lacked

examiner orientation of scanned images and the assignment of threshold sensitivity. The current study addressed these limitations by allowing examiners to manually orient images and set sensitivity thresholds. Importantly, examiners were unaware that intra-examiner reliability was being evaluated due to the use of duplicated images with random coding. The results revealed excellent intra-examiner reliability (ICC > 0.9 per Mattos et al.<sup>28</sup>) for all airway measurements in the MDCT × Amira (0.992–0.999) and CBCT × Amira (0.993–0.999) groups. Despite an intra-examiner ICC of 0.929 for NAV measured by one examiner (red circle) using Dolphin on CBCT, there was a 1593 mm<sup>3</sup> difference between measurements

**Table 7.** Extended

Patient 3			Patient 4			Patient 5		
MDCT × Amira Mean ± SD	MDCT × Dolphin Mean ± SD	Wilcoxon signed- rank test P value	MDCT × Amira Mean ± SD	MDCT × Dolphin Mean ± SD	Wilcoxon signed- rank test P value	MDCT × Amira Mean ± SD	MDCT × Dolphin Mean ± SD	Wilcoxon signed- rank test P value
33.91 ± 0.79	30.91 ± 1.25	<.001*	32.14 ± 0.79	32.88 ± 0.93	<.1	28.13 ± 0.7	28.05 ± 1.03	.6
20.73 ± 0.59	23.34 ± 1.77	<.001*	21.79 ± 0.49	25.07 ± 0.9	<.001*	18.79 ± 0.44	19.14 ± 1.42	.4
34.68 ± 0.78	35.15 ± 1.26	.3	35.79 ± 0.67	35.61 ± 1.08	.7	34.19 ± 0.57	32.97 ± 0.54	<.001*
34.78 ± 0.51	30.82 ± 1.3	<.001*	26.08 ± 0.62	25.38 ± 0.96	.037*	29.78 ± 0.7	29.08 ± 0.82	.035*
74.57 ± 0.56	76.9 ± 0.61	<.001*	71.04 ± 0.61	69.5 ± 0.79	<.001*	67.47 ± 0.62	69.26 ± 1.08	<.001*
30.68 ± 0.76	30.98 ± 0.95	.5	32.85 ± 0.8	29.34 ± 1.08	<.001*	24.51 ± 0.78	24.63 ± 0.94	.8
34.73 ± 0.97	34.9 ± 1.06	.6	37.48 ± 0.9	39.18 ± 1.13	.001*	29.58 ± 0.78	30.23 ± 0.89	.073*
51.73 ± 0.46	52.33 ± 0.71	.032*	49.7 ± 0.45	49.77 ± 0.57	.7	41.88 ± 0.61	41.94 ± 0.58	>.9
126.71 ± 0.69	125.17 ± 0.64	<.001*	121.88 ± 0.42	121.38 ± 1.32	.3	118.38 ± 0.63	116.13 ± 0.83	<.001*
11.63 ± 0.44	9.5 ± 0.54	<.001*	8.64 ± 0.44	8.31 ± 0.84	.12	8.53 ± 0.33	7.36 ± 0.79	<.001*
101.75 ± 0.58	101.16 ± 1.13	.2	95.94 ± 0.58	94.87 ± 0.81	.002*	93.71 ± 0.71	92.85 ± 0.74	.015*
26.07 ± 0.9	26.69 ± 1.08	.2	30.06 ± 0.57	30.09 ± 0.95	>.9	24.6 ± 0.68	24.36 ± 0.65	.4
71.2 ± 0.91	73.88 ± 1.63	<.001*	NA <sup>b</sup>	NA <sup>b</sup>	NA <sup>b</sup>	57.58 ± 1.01	60.1 ± 1.58	<.001*
78.57 ± 1.14	77.68 ± 1.45	.2	76.48 ± 0.56	77.16 ± 1.53	.12	75.7 ± 0.75	76.33 ± 1.13	.2
81.88 ± 0.89	81.45 ± 1.37	.4	79.95 ± 0.74	79.44 ± 1.08	.4	74.35 ± 0.97	76.8 ± 1.44	<.001*
84.71 ± 0.92	83.45 ± 1.04	.007*	74.13 ± 0.75	72.9 ± 1.14	.005*	76.29 ± 0.89	76.03 ± 1.11	.6
38.08 ± 0.48	37.98 ± 1.07	.9	23.88 ± 0.57	25.93 ± 1.16	<.001*	39.95 ± 0.76	38.36 ± 1	.001*
88.06 ± 0.62	89.61 ± 1.31	.003*	104.41 ± 0.82	105.25 ± 1.35	.10	104.93 ± 0.95	103.23 ± 1.37	.005*
85.57 ± 0.82	87.32 ± 1.06	<.001*	93.69 ± 0.89	95.18 ± 1.28	.007*	80.9 ± 0.98	81.7 ± 1.7	.4
138.16 ± 0.84	138.71 ± 1.25	.12	116.2 ± 0.68	113.79 ± 0.53	<.001*	123.25 ± 0.92	122.76 ± 1.46	.3
58.96 ± 0.86	60.31 ± 1.28	.012*	58.27 ± 0.7	57.35 ± 1.45	.10	58.84 ± 0.46	59.85 ± 1.02	.011*
NA <sup>c</sup>	NA <sup>c</sup>	NA <sup>c</sup>	709.33 ± 6.64	1301.17 ± 297.99	<.001*	4635.92 ± 28.59	5531.92 ± 506.34	<.001*
9610.58 ± 32.76	8319 ± 193.58	<.001*	7451.67 ± 28.85	8682.42 ± 431.97	<.001*	2450.58 ± 29.59	3425.75 ± 286.86	<.001*
33258.67 ± 32.81	35683.25 ± 561.85	<.001*	16155.75 ± 37.68	20312.08 ± 1411.1	<.001*	12678.25 ± 42.67	14982.75 ± 1381.89	<.001*
4348.33 ± 34.53	4584.42 ± 158.14	<.001*	2188.5 ± 28.32	2948.75 ± 42.9	<.001*	3152.08 ± 22.65	3971.5 ± 430.17	.078
357.33 ± 4.54	164.92 ± 9.34	<.001*	146.75 ± 4.65	179.33 ± 5.9	<.001*	106.83 ± 4.15	101 ± 35.15	<.001*

(9335 – 7,742 = 1,593 mm<sup>3</sup>) (Figure 2A). This indicated that simply reporting ICC ratings of “excellent,” or “almost perfect” agreement is insufficient to represent clinical reliability. Unexpectedly, some linear measurements of the hard tissue on the orthogonal planes and 3D surface rendering images exhibited lower intra- and inter-examiner reliability than airway measurements, even when using Amira. For instance, the intra-examiner error for ANW was as much as 4mm on CBCT (34.5 – 30.5 = 4 mm) using Dolphin (Figure 2B). The inter-examiner differences for PNW were as large as 2.9 mm (34.1 – 31.2 mm) using Amira on CBCT (red circle) and 4.3 mm (37.3 – 33 mm) using Dolphin (green circle) (Figure 2C). Since these measurements are common in

airway research, studies claiming treatment-induced craniofacial changes and airway improvements should be interpreted cautiously.

Treatment strategies for adult OSA, such as mandibular advancement devices, have shown effectiveness.<sup>29</sup> Conventional facial orthopedic treatments have proven effective for pediatric OSA.<sup>30</sup> However, the current study highlights the postural effect on upper airway structures/ dimensions, with measurements significantly smaller in MDCT scans compared to CBCT scans. Given the postural influence,<sup>31</sup> assessing airway dimensions using CBCT in the upright position for predicting supine-position-related sleep apnea disorders requires further validation.

**Table 8.** Average Data Obtained by Amira and Dolphin on Cone-Beam Computed Tomography (CBCT) Images For Each Patient

CBCT	Variable	Patient-1			Patient-2		
		CBCT ± Amira Mean ± SD	CBCT ± Dolphin Mean ± SD	Wilcoxon signed-rank test P value	CBCT ± Amira Mean ± SD	CBCT ± Dolphin Mean ± SD	Wilcoxon signed-rank test P value
Linear measurements on the orthogonal planes	ANW	32.54 ± 0.6	32.38 ± 1.24	.4	NA <sup>a</sup>	NA <sup>a</sup>	NA <sup>a</sup>
	ANFW	21.53 ± 0.66	17.97 ± 1.29	<.001*	NA <sup>a</sup>	NA <sup>a</sup>	NA <sup>a</sup>
	PNW	32.22 ± 0.91	34.16 ± 1.23	<.001*	NA <sup>a</sup>	NA <sup>a</sup>	NA <sup>a</sup>
	PNFW	28.78 ± 0.72	24.61 ± 0.59	<.001*	NA <sup>a</sup>	NA <sup>a</sup>	NA <sup>a</sup>
	EMW	60.94 ± 0.71	63.13 ± 0.65	<.001*	NA <sup>a</sup>	NA <sup>a</sup>	NA <sup>a</sup>
	PW	33.85 ± 0.95	31.4 ± 1.54	<.001*	31 ± 0.86	34.55 ± 1.5	<.001*
	Inter-Mpa	37.35 ± 0.9	42.69 ± 0.97	<.001*	42.26 ± 0.81	41.41 ± 1.23	.094
Linear measurements on the three-dimen- sional (3D) surface rendering images	Inter-Mcf	46.64 ± 0.53	45.08 ± 0.71	<.001*	NA <sup>a</sup>	NA <sup>a</sup>	NA <sup>a</sup>
	ZTUR-l	133.26 ± 0.61	132.51 ± 1.33	0.11	136.59 ± 0.8	137.61 ± 0.79	.007*
	FMR-l	7.58 ± 0.35	7.39 ± 0.55	0.3	NA <sup>a</sup>	NA <sup>a</sup>	NA <sup>a</sup>
	FZR-l	103.76 ± 0.64	104.19 ± 0.97	0.2	105.71 ± 0.52	108.53 ± 1.11	<.001*
	INCR-l	26.84 ± 0.63	25.43 ± 0.59	<.001*	25.6 ± 0.33	26.5 ± 0.82	.003*
	ZMLR-l	73.15 ± 0.7	75.68 ± 2.06	0.002*	NA <sup>a</sup>	NA <sup>a</sup>	NA <sup>a</sup>
Lateral cephalometric analysis	ZMLR-l	87.29 ± 0.77	84.69 ± 1.46	<.001*	NA <sup>a</sup>	NA <sup>a</sup>	NA <sup>a</sup>
	SNA	91.01 ± 0.74	92.65 ± 0.94	<.001*	78.15 ± 0.81	77.72 ± 1.12	.2
	SNB	86.09 ± 0.7	85.76 ± 0.77	0.3	79.03 ± 0.8	78.47 ± 1.76	.019*
	SNGoGn	33.58 ± 0.83	31.6 ± 1.19	<.001*	38.7 ± 0.72	38.24 ± 0.98	.3
	L	101.68 ± 1.06	99.75 ± 0.85	<.001*	124.93 ± 0.54	125.92 ± 1.34	.056
	Co-A	96.99 ± 0.83	98.71 ± 1.49	0.005*	89.25 ± 0.71	88.04 ± 1.57	.040*
Airway analysis	Co-Gn	139.43 ± 1.03	137.38 ± 1.25	0.001*	134.54 ± 0.84	134.25 ± 1.28	.5
	TOH	63.78 ± 0.71	63.15 ± 1.07	0.2	75.8 ± 0.67	76.59 ± 1.31	.2
	IAV	8763.83 ± 28.36	11279.58 ± 1383.33	<.001*	NA <sup>c</sup>	NA <sup>c</sup>	NA <sup>c</sup>
	NAV	4650 ± 35.38	5494.17 ± 214.78	<.001*	3448.25 ± 17.18	3894.92 ± 273.84	<.001*
	OAV	22975.83 ± 42.06	20788.33 ± 658.27	<.001*	44780.33 ± 25.68	41409.33 ± 1737.64	<.001*
	HAV	7532.75 ± 22.4	8927.08 ± 198.28	<.001*	NA <sup>d</sup>	NA <sup>d</sup>	NA <sup>d</sup>
	MCA	280 ± 6.21	212.83 ± 27.17	<.001*	318.75 ± 3.79	352.58 ± 13.93	<.001*

\* P value < .05 indicates statistical significance.

<sup>a</sup> Data was not available because patient had previous midface reconstruction.

<sup>b</sup> Data was not available because the upper border of the zygomaticomaxillary suture of this patient was not obvious.

<sup>c</sup> Data was not available because there was no intraoral airway space for this patient.

<sup>d</sup> Data was not available because the field of view was too small to include the lower boundary of the hypopharyngeal airway.

<sup>e</sup> ANFW indicates anterior nasal floor width; ANW, anterior nasal width; CBCT, cone-beam computed tomography; CI, confidence interval; Co-A, Condylion to point A; Co-Gn, Condylion to Gnathion; EMW, external maxillary width; FMR-l, frontomaxillary suture right to left; FZR-l, frontozygomatic right to left; HAV, hypopharyngeal airway volume; IAV, intraoral airway volume; ICC, intraclass correlation coefficients; INCR-l, inner nasal contour point right to left; Inter-Mcf, intermolar width at the first molar central fossa level; Inter-Mpa, intermolar width at the first molar palatal apex level; L, lordosis angle; MCA, minimum cross-sectional area in oropharynx; NA, not available; NAV, nasopharyngeal airway volume; OAV, oropharyngeal airway volume; PNFW, posterior nasal floor width; PNW, posterior nasal width; PW, palatal width; SD, standard deviation; SNA, Sella-Nasion-subspinale angle; SNB, Sella-Nasion-supramentale angle; SNGoGn: Sella-Nasion-Gonion-Gnathion angle; TOH, total oropharynx height; ZMLR-l, zygomaticomaxillary lower right to left; ZMUR-l, Zygomaticomaxillary upper right to left; ZTUR-l, zygomaticotemporal suture upper right to left.

## Limitations

Limitations of this study included a small sample size and a retrospective design relying on existing databases. A database search for adult patients who had undergone CBCT and MDCT head and neck scans within a year, excluding those who received treatment affecting craniofacial structures during that period, yielded only five subjects meeting the inclusion criteria. Nonetheless, this limited sample size may reflect adherence to the “as low as reasonably achievable” (ALARA) principle in patient treatment. Additionally, the comparison involved

only one MDCT, one CBCT, and two imaging software packages, limiting generalizability to other scanner models and software. The results of this study only apply to the present imaging protocols with the same scanner models. For example, the slice thickness of MDCT in this study was 1.2 mm, while the voxel of CBCT was 0.25 mm. The thickness of each slice between the two modalities was not equal, which may have affected the accuracy and reliability of the research results. As the slice thickness of MDCT was large, the imaging quality might have been underestimated.

**Table 8.** Extended

Patient-3			Patient-4			Patient-5		
CBCT ± Amira Mean ± SD	CBCT ± Dolphin Mean ± SD	Wilcoxon signed- rank test P value	CBCT ± Amira Mean ± SD	CBCT ± Dolphin Mean ± SD	Wilcoxon signed- rank test P value	CBCT ± Amira Mean ± SD	CBCT ± Dolphin Mean ± SD	Wilcoxon signed- rank test P value
34.08 ± 0.65	30.88 ± 1.02	<.001*	31.25 ± 0.76	30.54 ± 0.73	.052	28.79 ± 0.55	30.31 ± 1.16	
20.18 ± 0.64	20.03 ± 1.35	.5	21.36 ± 0.43	25.08 ± 1.73	<.001*	18.83 ± 0.5	18.66 ± 0.68	.7
35.11 ± 0.53	36.72 ± 1.01	<.001*	36.35 ± 0.68	36.08 ± 1.17	.6	34.43 ± 1.07	33.88 ± 0.89	.3
35.18 ± 0.48	29.92 ± 0.86	<.001*	26.74 ± 0.6	27.81 ± 0.99	.011*	30 ± 0.59	28.65 ± 1.17	.004*
74.2 ± 0.72	76.48 ± 1.16	<.001*	71.18 ± 0.7	70.6 ± 1.21	.15	67.64 ± 0.75	68.92 ± 0.89	.003*
29.73 ± 0.98	29.08 ± 0.92	.10	32.13 ± 0.86	29.34 ± 1.32	<.001*	25.38 ± 0.58	23 ± 1.63	<.001*
34.67 ± 0.66	33.08 ± 2.15	.003*	37.84 ± 0.69	35.98 ± 1.7	.005*	29.92 ± 0.6	28.04 ± 1.03	<.001*
51.73 ± 0.36	51.28 ± 0.74	.077	49.21 ± 0.33	48.98 ± 2.92	.12	41.93 ± 0.58	41.51 ± 1.13	.6
127.27 ± 0.61	125.95 ± 1.22	.002*	122.9 ± 0.52	119.68 ± 0.92	<.001*	117.39 ± 1.04	115.29 ± 1.04	<.001*
11.28 ± 0.47	9.68 ± 0.68	<.001*	8.48 ± 0.34	8.59 ± 1.04	.2	8.43 ± 0.51	8.58 ± 0.64	.5
101 ± 0.55	100.52 ± 0.89	.3	95.14 ± 0.37	96.03 ± 1.63	.064	93.3 ± 0.65	93.27 ± 0.89	.9
26.13 ± 0.48	26.76 ± 1.65	.5	29.63 ± 0.82	28.63 ± 1.38	.056	24.94 ± 0.86	23.63 ± 0.79	.003*
71.1 ± 0.78	68.8 ± 1.91	.004*	NA <sup>b</sup>	NA <sup>b</sup>	NA <sup>b</sup>	58.5 ± 1.08	59.88 ± 1.63	.019*
78.61 ± 1.28	79.23 ± 1.45	.4	77.52 ± 1.01	74.83 ± 1.55	<.001*	75.42 ± 0.91	74.01 ± 1.44	.030*
81.73 ± 0.72	82.07 ± 0.94	.3	79.82 ± 0.66	80.63 ± 1.35	.032*	74.22 ± 0.73	75.74 ± 0.79	<.001*
84.14 ± 0.82	85.2 ± 0.73	.003*	74.88 ± 0.61	75.41 ± 0.73	.077	75.86 ± 0.76	76.43 ± 0.67	.14
37.64 ± 0.85	34.91 ± 0.8	<.001*	22.78 ± 0.73	21.65 ± 1.35	.028*	40.04 ± 0.86	40.02 ± 0.96	>.9
91.6 ± 0.59	90.9 ± 1.14	.15	104.58 ± 0.77	105.3 ± 1.57	.3	106.54 ± 0.75	102.98 ± 0.94	<.001*
84.65 ± 0.95	86.82 ± 1.57	.001*	92.4 ± 0.95	95.63 ± 1.32	<.001*	80.25 ± 0.81	79.08 ± 1.33	.015*
139.14 ± 3.33	139.05 ± 1.1	.13	116.8 ± 1.11	118.76 ± 1.07	.001*	123.28 ± 0.9	121.66 ± 1.29	.002*
59.13 ± 0.46	62.07 ± 0.87	<.001*	58.14 ± 0.53	58.52 ± 1.41	.5	57.62 ± 0.72	59.05 ± 0.79	<.001*
1472.75 ± 16.33	2392.75 ± 195.5	<.001*	NA <sup>c</sup>	NA <sup>c</sup>	NA <sup>c</sup>	9049.58 ± 25.77	6598.5 ± 906.63	<.001*
9087.83 ± 53.73	8490.58 ± 201.55	<.001*	7542.5 ± 30.13	7953.17 ± 258.39	<.001*	3749.25 ± 30.22	8272.58 ± 626.49	<.001*
41396.17 ± 270.48	43123.08 ± 1225.48	<.001*	17274.67 ± 34.54	17701.17 ± 1154.66	.8	15498.33 ± 52.68	18000.58 ± 1599.41	<.001*
6112.5 ± 13.13	6567.58 ± 225.97	<.001*	NA <sup>d</sup>	NA <sup>d</sup>	NA <sup>d</sup>	4946.42 ± 25.49	5806.42 ± 501.46	<.001*
388.25 ± 4.9	263.83 ± 28.5	<.001*	206.75 ± 5.72	202.58 ± 8.85	.3	235.75 ± 4.54	101.25 ± 6.9	<.001*

**CONCLUSIONS**

Within the limitations of this study, the following conclusions can be drawn:

- Dolphin was deemed unreliable for airway analysis, while proper training with software supporting HU calibration, such as Amira, could yield relatively reliable airway measurements.
- Airway volumes were significantly reduced on MDCT scans compared to CBCT, except for IAV.
- The undesirable reliability found for skeletal measurements precludes using CT to correlate craniofacial changes with airway dimensions.

**REFERENCES**

1. Angelopoulos C, Scarfe WC, Farman AG. A comparison of maxillofacial CBCT and medical CT. *Atlas Oral Maxillofac Surg Clin North Am.* 2012;20(1):1–17.
2. Proffit WR. *Contemporary Orthodontics.* 6th ed. Philadelphia, IL: Elsevier; 2018.
3. Guijarro-Martínez R, Swennen GR. Cone-beam computerized tomography imaging and analysis of the upper airway: a systematic review of the literature. *Int J Oral Maxillofac Surg.* 2011;40(11):1227–1237.
4. De Felice F, Di Carlo G, Saccucci M, Tombolini V, Polimeni A. Dental cone beam computed tomography in children: clinical effectiveness and cancer risk due to radiation exposure. *Oncology.* 2019;96(4):173–178.

**Table 9.** Average Data Obtained by Amira and Dolphin on Multidetector Computed Tomography (MDCT) and cone-beam computed tomography (CBCT) images of the dry skull.

Skull (gold standard)	Variable	MDCT × Amira Mean ± SD	MDCT × Dolphin Mean ± SD	Wilcoxon signed-rank test P value	CBCT × Amira Mean ± SD	CBCT × Dolphin Mean ± SD	Wilcoxon signed-rank test P value
Linear measurements on the orthogonal planes	ANW	31.75 ± 0.3	31.09 ± 0.69	.003*	30.22 ± 0.39	30.45 ± 0.44	.2
	ANFW	27.27 ± 0.49	26.74 ± 0.64	.031*	26.17 ± 0.33	25.8 ± 0.81	.022*
	PNW	36.49 ± 0.73	36.92 ± 0.46	.2	36.53 ± 0.69	36.18 ± 0.45	.10
	PNFW	31.5 ± 0.76	31.05 ± 0.48	.077	31.38 ± 0.47	31.68 ± 0.59	.13
	EMW	66.95 ± 0.57	67.53 ± 0.51	.024*	67.35 ± 0.51	67.23 ± 0.47	.7
	PW	30.96 ± 0.47	31.06 ± 0.61	>.9	31.79 ± 0.51	31.42 ± 0.78	.2
	Inter-Mpa	37.68 ± 0.63	38.19 ± 0.54	.067	37.24 ± 0.5	38.27 ± 0.59	<.001*
Linear measurements on the three-dimensional (3D) surface rendering images	Inter-Mcf	46.61 ± 0.6	47.24 ± 0.36	.008*	46.78 ± 0.48	47.03 ± 0.37	.10
	ZTUR-l	108.23 ± 0.49	108.03 ± 0.41	.2	109.58 ± 0.6	109.13 ± 0.73	.3
	FMR-l	9.91 ± 0.38	9.66 ± 0.52	.15	9.83 ± 0.31	9.77 ± 0.59	>.9
	FZR-l	90.11 ± 0.45	90.23 ± 0.55	.6	91.06 ± 0.42	90.66 ± 0.66	.10
	INCR-l	26.98 ± 0.45	27.88 ± 0.38	<.001*	27.13 ± 0.44	27.27 ± 0.61	.6
Lateral cephalometric analysis	ZMUR-l	60.73 ± 1	62.87 ± 0.52	<.001*	60.33 ± 0.92	61.98 ± 0.62	<.001*
	ZMLR-l	74.03 ± 0.65	75.46 ± 0.78	<.001*	73.81 ± 1.27	73.74 ± 0.64	.5
	SNA	84.18 ± 0.6	83.83 ± 0.93	.4	83.94 ± 0.61	84.82 ± 0.69	.005*
	SNB	77.93 ± 0.84	77.79 ± 0.99	.8	77.78 ± 0.87	78.7 ± 0.66	.008*
	SNGoGn	31.04 ± 0.43	31.91 ± 0.67	.003*	31.48 ± 0.57	32.21 ± 0.37	.005*
Co-A	83.57 ± 0.42	86.03 ± 0.61	<.001*	82.74 ± 0.62	85.76 ± 0.73	<.001*	
Co-Gn	113.02 ± 0.61	115.33 ± 0.55	<.001*	111.88 ± 0.54	114.42 ± 0.5	<.001*	

\* P value < .05 indicates statistical significance.

<sup>a</sup> ANFW indicates anterior nasal floor width; ANW, anterior nasal width; CBCT, cone-beam computed tomography; CI, confidence interval; Co-A, Condylion to point A; Co-Gn, Condylion to Gnathion; EMW, external maxillary width; FMR-l, frontomaxillary suture right to left; FZR-l, frontozygomatic right to left; HAV: HAV, hypopharyngeal airway volume; IAV, intraoral airway volume; ICC, intraclass correlation coefficients; INCR-l, inner nasal contour point right to left; Inter-Mcf, intermolar width at the first molar central fossa level; Inter-Mpa, intermolar width at the first molar palatal apex level; L, lordosis angle; MCA, minimum cross-sectional area in oropharynx; MDCT, multi-detector computed tomography; NAV, nasopharyngeal airway volume; OAV, oropharyngeal airway volume; PNFW, posterior nasal floor width; PNW, posterior nasal width; PW, palatal width; SD, standard deviation; SNA, Sella-Nasion-subspinale angle; SNB, Sella-Nasion-supramentale angle; SNGoGn: Sella-Nasion-Gonion-Gnathion angle; TOH, total oropharynx height; ZMLR-l, zygomaticomaxillary lower right to left; ZMUR-l, Zygomaticomaxillary upper right to left; ZTUR-l, zygomaticotemporal suture upper right to left.

- Pauwels R, Jacobs R, Singer SR, Mupparapu M. CBCT-based bone quality assessment: are Hounsfield units applicable? *Dentomaxillofac Radiol.* 2015;44(1):20140238.
- Eguren M, Holguin A, Diaz K, et al. Can gray values be converted to Hounsfield units? A systematic review. *Dentomaxillofac Radiol.* 2022;51(1):20210140.
- Pauwels R, Nackaerts O, Bellaiche N, et al. Variability of dental cone beam CT grey values for density estimations. *Br J Radiol.* 2013;86(1021):20120135.
- Yamashina A, Tanimoto K, Sutthiprapaporn P, Hayakawa Y. The reliability of computed tomography (CT) values and dimensional measurements of the oropharyngeal region using cone beam CT: comparison with multidetector CT. *Dentomaxillofac Radiol.* 2008;37(5):245–251.
- Kim M, Huh KH, Yi WJ, Heo MS, Lee SS, Choi SC. Evaluation of accuracy of 3D reconstruction images using multi-detector CT and cone-beam CT. *Imaging Sci Dent.* 2012;42(1):25–33.
- Freire-Maia B, Machado VD, Valerio CS, Custodio AL, Manzi FR, Junqueira JL. Evaluation of the accuracy of linear measurements on multi-slice and cone beam computed tomography scans to detect the mandibular canal during bilateral sagittal split osteotomy of the mandible. *Int J Oral Maxillofac Surg.* 2017;46(3):296–302.
- Loubele M, Van Assche N, Carpentier K, et al. Comparative localized linear accuracy of small-field cone-beam CT and multislice CT for alveolar bone measurements. *Oral Surg Oral Med Oral Pathol Oral Radiol Endod.* 2008;105(4):512–518.
- Naser AZ, Mehr BB. A comparative study of accuracy of linear measurements using cone beam and multi-slice computed tomographies for evaluation of mandibular canal location in dry mandibles. *Dent Res J (Isfahan).* 2013;10(1):15–19.
- Chen H, van Eijnatten M, Aarab G, et al. Accuracy of MDCT and CBCT in three-dimensional evaluation of the oropharynx morphology. *Eur J Orthod.* 23 2018;40(1):58–64.
- Zimmerman JN, Lee J, Pliska BT. Reliability of upper pharyngeal airway assessment using dental CBCT: a systematic review. *Eur J Orthod.* 1 2017;39(5):489-496.
- Pangrazio-Kulbersh V, Wine P, Haughey M, Pajtas B, Kaczynski R. Cone beam computed tomography evaluation of changes in the naso-maxillary complex associated with two types of maxillary expanders. *Angle Orthod.* 2012;82(3):448–457.
- Venezia P, Nucci L, Moschitto S, et al. Short-term and long-term changes of nasal soft tissue after rapid maxillary expansion (RME) with tooth-borne and bone-borne devices. A CBCT Retrospective Study. *Diagnostics (Basel).* Mar 31 2022;12(4).

**Table 10.** Regression Models for Variables in the Category of “Linear Measurements on the Orthogonal Planes”

Variable	ANW			ANW			ANFW			PNW		
	Estimated value	Standard error	P value	Estimated value	Standard error	P value	Estimated value	Standard error	P value	Estimated value	Standard error	P value
Intercept term	31.070	0.364	<.001*	20.780	0.405	<.001*	34.941	0.280	<.001*	27.947	0.513	<.001*
Imaging modality (MDCT vs CBCT)	-0.044	0.350	.900	1.624	0.390	<.001*	-0.489	0.269	.070	0.241	0.493	.625
Measurement software (Amira vs Dolphin)	0.529	0.350	.040*	-0.143	0.390	.715	-0.554	0.269	.040*	2.285	0.493	<.001*
Type of subject (skull vs patient)	-0.852	0.505	.032*	4.915	0.562	<.001*	1.289	0.388	.001*	3.569	0.712	<.001*
Examiner-2	0.003	0.404	.995	-0.603	0.450	.182	0.200	0.310	.520	-0.070	0.570	.902
Examiner-3	-0.135	0.404	.739	-0.200	0.450	.657	0.333	0.310	.285	-0.278	0.570	.627
Examiner-4	0.148	0.404	.716	-0.200	0.450	.657	0.518	0.310	.096	0.060	0.570	.916
Examiner-5	-0.003	0.404	.995	-0.238	0.450	.598	0.108	0.310	.729	-0.458	0.570	.423
Examiner-6	0.048	0.404	.907	-0.290	0.450	.520	0.068	0.310	.828	-0.028	0.570	.962
Imaging modality × measurement software	-0.053	0.467	.909	-1.240	0.519	.018	0.230	0.358	.521	-0.595	0.658	.367
Imaging modality × Type of subject	1.129	0.583	.054	0.038	0.649	.954	0.712	0.448	.113	-0.290	0.822	.725
Measurement software × Type of subject	-0.269	0.583	.645	1.271	0.649	.052	0.534	0.448	.234	-1.983	0.822	.017*

\* P value < .05 indicates statistical significance.

<sup>a</sup> ANFW indicates anterior nasal floor width; ANW, anterior nasal width; CBCT, cone-beam computed tomography; EMW, external maxillary width; Inter-Mcf, intermolar width at the first molar central fossa level; Inter-Mpa, intermolar width at the first molar palatal apex level; MDCT, multi-detector computed tomography; PNFW, posterior nasal floor width; PNW, posterior nasal width; PW, palatal width.

17. Kavand G, Lagravere M, Kula K, Stewart K, Ghoneima A. Retrospective CBCT analysis of airway volume changes after bone-borne vs tooth-borne rapid maxillary expansion. *Angle Orthod.* 2019;89(4):566–574.
18. Yilmaz BS, Kucukkeles N. Skeletal, soft tissue, and airway changes following the alternate maxillary expansions and constrictions protocol. *Angle Orthod.* 2014;84(5):868–877.
19. Cho AR, Park JH, Moon W, Chae JM, Kang KH. Short-term effects of microimplant-assisted rapid palatal expansion on the circummaxillary sutures in skeletally mature patients: a cone-beam computed tomography study. *Am J Orthod Dentofacial Orthop.* 2022;161(2):e187–e197.
20. Angelieri F, Franchi L, Cevidanes LHS, Hino CT, Nguyen T, McNamara JA, Jr. Zygomaticomaxillary suture maturation: a predictor of maxillary protraction? Part I - A classification method. *Orthod Craniofac Res.* 2017;20(2):85–94.
21. Almuzian M, Ju X, Almukhtar A, Ayoub A, Al-Muzian L, McDonald JP. Does rapid maxillary expansion affect nasopharyngeal airway? A prospective Cone Beam Computerised Tomography (CBCT) based study. *Surgeon.* 2018;16(1):1–11.
22. Guijarro-Martinez R, Swennen GR. Three-dimensional cone beam computed tomography definition of the anatomical subregions of the upper airway: a validation study. *Int J Oral Maxillofac Surg.* 2013;42(9):1140–1149.
23. Iwasaki T, Suga H, Yanagisawa-Minami A, et al. Relationships among tongue volume, hyoid position, airway volume and maxillofacial form in paediatric patients with Class-I, Class-II and Class-III malocclusions. *Orthod Craniofac Res.* 2019;22(1):9–15.
24. Landis JR, Koch GG. The measurement of observer agreement for categorical data. *Biometrics.* 1977;33(1):159–174.
25. Nimbalkar S. Accuracy of volumetric analysis software packages in assessment of tooth volume using CBCT. *Loma Linda University Electronic Theses, Dissertations & Projects.* 2016; 400. <https://scholarsrepository.llu.edu/etd/400>.
26. Weissheimer A, Menezes LM, Sameshima GT, Enciso R, Pham J, Grauer D. Imaging software accuracy for 3-dimensional analysis of the upper airway. *Am J Orthod Dentofacial Orthop.* 2012;142(6):801–813.
27. de Water VR, Saridin JK, Bouw F, Murawska MM, Koudstaal MJ. Measuring upper airway volume: accuracy and reliability of Dolphin 3D software compared to manual segmentation in craniostenosis patients. *J Oral Maxillofac Surg.* 2014;72(1):139–144.
28. Mattos CT, Cruz CV, da Matta TC, et al. Reliability of upper airway linear, area, and volumetric measurements in cone-beam computed tomography. *Am J Orthod Dentofacial Orthop.* 2014;145(2):188–197.
29. Gao YN, Wu YC, Lin SY, Chang JZ, Tu YK. Short-term efficacy of minimally invasive treatments for adult obstructive sleep apnea: A systematic review and network meta-analysis of randomized controlled trials. *J Formos Med Assoc.* 2019;118(4):750–765.
30. Lin SY, Su YX, Wu YC, Chang JZ, Tu YK. Management of paediatric obstructive sleep apnoea: a systematic review and network meta-analysis. *Int J Paediatr Dent.* 2020;30(2):156–170.
31. Sutthiprapaporn P, Tanimoto K, Ohtsuka M, Nagasaki T, Iida Y, Katsumata A. Positional changes of oropharyngeal structures due to gravity in the upright and supine positions. *Dentomaxillofac Radiol.* 2008;37(3):130–135.

**Table 10.** Extended

PNFW			EMW			PW			Inter-Mpa		
Estimated value	Standard error	<i>P</i> value	Estimated value	Standard error	<i>P</i> value	Estimated value	Standard error	<i>P</i> value	Estimated value	Standard error	<i>P</i> value
69.851	0.885	<.001*	29.550	0.593	<.001*	36.658	0.764	<.001*	46.655	0.711	<.001*
0.275	0.850	.746	0.861	0.567	.130	0.399	0.732	.586	1.016	0.683	.138
-1.216	0.850	.154	0.926	0.567	.104	0.066	0.732	.928	0.603	0.683	.378
-2.363	1.227	.050*	1.898	0.889	.034*	1.724	1.146	.134	0.165	0.985	.868
-0.428	0.981	.664	-0.269	0.663	.685	-0.671	0.854	.433	-0.07	0.788	.929
0.123	0.981	.901	0.002	0.663	.998	-0.521	0.854	.543	0.108	0.788	.892
-0.313	0.981	.751	0.094	0.663	.888	-0.21	0.854	.806	0.118	0.788	.882
0.065	0.981	.947	-0.179	0.663	.787	-0.469	0.854	.584	0.093	0.788	.907
-0.095	0.981	.923	-0.065	0.663	.922	-0.333	0.854	.697	0.273	0.788	.730
-0.082	1.133	.943	-0.619	0.765	.419	-0.533	0.986	.589	-0.840	0.910	.357
-0.268	1.417	.850	-1.143	1.027	.266	0.03	1.323	.982	-0.554	1.138	.627
1.099	1.417	.439	-0.475	1.027	.644	-0.662	1.323	.617	-0.575	1.138	.614

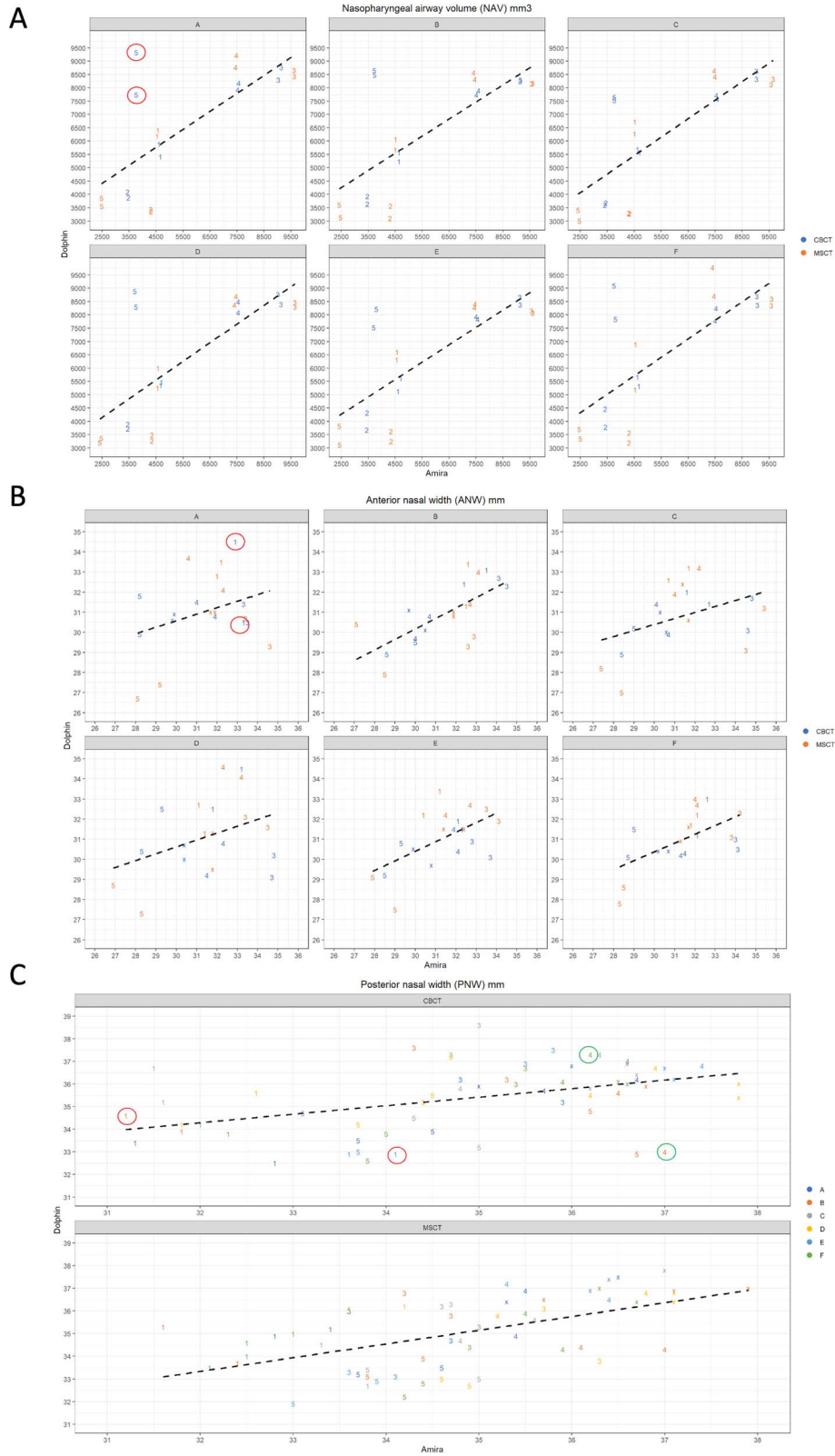


**Figure 2.** Intra-examiner reliability for nasopharyngeal airway volume (A) and anterior nasal width (B). Inter-examiner reliability for posterior nasal width (C). Letters A to F: six examiners. Numbers 1 to 5: individual patients. The letter 'x' dry skull. MSCT = MDCT. Black dashed line: regression line.

**Table 11.** Regression Models for Variables in the Category of “Linear Measurements on the Three-Dimensional (3D) Surface Rendering Images”

Variable	ZTUR-I			ZMUR-I		
	Estimated value	Standard error	P value	Estimated value	Standard error	P value
Intercept term	126.050	1.284	< .001*	68.126	1.365	< .001*
Imaging modality (MDCT vs CBCT)	0.574	1.229	.641	0.627	1.319	.635
Measurement software (Amira vs Dolphin)	1.249	1.229	.310	-0.532	1.319	.687
Type of subject (skull vs patient)	-17.147	1.926	< .001*	-6.135	1.727	< .001*
Examiner-2	0.096	1.436	.947	0.225	1.496	.881
Examiner-3	0.121	1.436	.933	-0.256	1.496	.864
Examiner-4	0.448	1.436	.755	0.100	1.496	.947
Examiner-5	0.188	1.436	.896	-0.100	1.496	.947
Examiner-6	0.171	1.436	.905	-0.022	1.496	.988
Imaging modality × measurement software	-0.574	1.658	.730	-0.748	1.727	.665
Imaging modality × Type of subject	-1.554	2.224	.485	0.251	1.994	.900
Measurement software × Type of subject	-0.621	2.224	.780	-0.899	1.994	.653

\* P value < .05 indicates statistical significance.

<sup>a</sup>CBCT, cone-beam computed tomography; FMr-I, frontomaxillary suture right to left; FZr-I, frontozygomatic right to left; INCr-I, inner nasal contour point right to left; MDCT, multidetector computed tomography; ZMLr-I, zygomaticomaxillary lower right to left; ZMUR-I, zygomaticomaxillary upper right to left; ZTUR-I, zygomaticotemporal suture upper right to left.

**Table 12.** Regression Models for Variables in the Category of “Lateral Cephalometric Analysis”

Variable	SNA			SNB		
	Estimated value	Standard error	P value	Estimated value	Standard error	P value
Intercept term	81.918	0.917	< .001	80.121	0.785	< .001*
Imaging modality (MDCT vs CBCT)	-0.952	0.878	.279	-0.909	0.752	.228
Measurement software (Amira vs Dolphin)	-0.820	0.878	.351	-0.274	0.752	.716
Type of subject (skull vs patient)	2.929	1.375	.034*	-1.614	1.178	.172
Examiner-2	-0.156	1.025	.879	0.244	0.878	.781
Examiner-3	-0.081	1.025	.937	0.338	0.878	.701
Examiner-4	-0.427	1.025	.677	-0.079	0.878	.928
Examiner-5	-0.025	1.025	.981	0.229	0.878	.794
Examiner-6	-0.123	1.025	.905	0.113	0.878	.898
Imaging modality × measurement software	0.864	1.183	.466	0.685	1.014	.500
Imaging modality × Type of subject	0.170	1.588	.915	0.104	1.360	.939
Measurement software × Type of subject	0.122	1.588	.939	-0.389	1.360	.775

\* P value < .05 indicates statistical significance.

CBCT, cone-beam computed tomography; Co-A, Condylion to Point A; Co-Gn, Condylion to Gnathion; L, lordosis angle; MDCT, multi-detector computed tomography; NA, not available; SNA, Sella-Nasion-subspinale angle; SNB, Sella-Nasion-supramentale angle; SNGoGn, Sella-Nasion-Gonion-Gnathion angle.

**Table 11.** Extended

ZMLr-I			FMr-I			FZr-I			INCr-I		
Estimated value	Standard error	P value	Estimated value	Standard error	P value	Estimated value	Standard error	P value	Estimated value	Standard error	P value
78.272	0.926	<.001*	8.543	0.246	<.001*	100.462	0.872	<.001*	26.262	0.335	<.001*
2.136	0.890	.017*	-0.521	0.237	.029*	-0.401	0.835	.631	0.754	0.320	.019*
1.438	0.890	.107	0.463	0.237	.050*	-0.618	0.835	.460	0.441	0.320	.170
-4.649	1.284	<.001*	1.404	0.342	<.001*	-9.526	1.308	<.001*	1.081	0.502	.032*
0.168	1.027	.871	0.040	0.273	.884	-0.123	0.975	.900	0.192	0.374	.609
-0.223	1.027	.829	-0.043	0.273	.877	0.231	0.975	.813	-0.229	0.374	.541
0.125	1.027	.903	0.035	0.273	.898	-0.067	0.975	.946	-0.215	0.374	.567
-0.138	1.027	.894	-0.063	0.273	.819	-0.127	0.975	.896	-0.063	0.374	.867
-0.185	1.027	.857	-0.100	0.273	.715	0.033	0.975	.973	-0.129	0.374	.730
-2.228	1.186	.062	0.750	0.315	.018*	0.607	1.126	.590	-0.724	0.432	.095
-0.097	1.483	.948	0.096	0.394	.808	-0.569	1.510	.707	-0.151	0.580	.795
-1.049	1.483	.480	-0.713	0.394	.072	0.423	1.510	.780	-0.629	0.580	.279

**Table 12.** Extended

SNGoGn			L			Co-A			Co-Gn		
Estimated value	Standard error	P value	Estimated value	Standard error	P value	Estimated value	Standard error	P value	Estimated value	Standard error	P value
33.457	1.019	<.001*	105.326	1.949	<.001*	89.339	1.038	<.001*	130.242	1.582	<.001*
1.78	0.975	.069*	-1.55	1.837	.400	0.172	0.994	.863	-0.135	1.514	.929
1.118	0.975	.253	0.897	1.837	.626	-0.968	0.994	.331	0.380	1.514	.802
-1.51	1.528	.324	NA	NA	NA	-3.961	1.557	.012*	-15.918	2.372	<.001*
0.021	1.139	.985	-0.138	2.25	.951	0.569	1.161	.624	-0.206	1.768	.907
-0.19	1.139	.868	-0.458	2.25	.839	0.248	1.161	.831	-0.098	1.768	.956
-0.277	1.139	.808	-0.553	2.25	.806	0.329	1.161	.777	0.031	1.768	.986
-0.052	1.139	.964	-0.525	2.25	.816	0.438	1.161	.707	0.244	1.768	.890
-0.106	1.139	.926	-0.475	2.25	.833	0.379	1.161	.744	0.013	1.768	.994
-1.442	1.315	.274	-1.228	2.598	.637	0.294	1.34	.826	-0.206	2.042	.920
-1.355	1.764	.443	NA	NA	NA	0.210	1.798	.907	1.242	2.739	.651
-1.218	1.764	.491	NA	NA	NA	-1.908	1.798	.289	-2.740	2.739	.318

Downloaded from https://prime-pdf-watemark.prime-prod.pubfactory.com/ at 2025-07-01 via free access

**Table 13.** Regression Models for Variables in the Category of "Airway Analysis"

Variable	TOH			IAV		
	Estimated value	Standard error	<i>P</i> value	Estimated value	Standard error	<i>P</i> value
Intercept term	63.885	1.271	< .001*	6723.160	1154.560	< .001*
Imaging modality (MDCT vs CBCT)	-1.275	1.199	.289	21.990	1061.210	.983
Measurement software (Amira vs Dolphin)	-0.982	1.199	.414	-328.220	1134.480	.773
Type of subject (skull vs patient)	NA	NA	NA	NA	NA	NA
Examiner-2	-0.003	1.468	.999	121.070	1286.380	.925
Examiner-3	0.04	1.468	.978	-31.000	1286.380	.981
Examiner-4	0.078	1.468	.958	-114.430	1286.380	.929
Examiner-5	-0.233	1.468	.874	139.180	1286.380	.914
Examiner-6	0.058	1.468	.969	87.860	1286.380	.946
Imaging modality × measurement software	1.413	1.695	.405	392.200	1500.780	.794
Imaging modality × Type of subject	NA	NA	NA	NA	NA	NA
Measurement software × Type of subject	NA	NA	NA	NA	NA	NA

\* *P* value < .05 indicates statistical significance.

<sup>a</sup> CBCT, cone-beam computed tomography; HAV, hypopharyngeal airway volume; IAV, Intraoral airway volume; MCA, minimum cross-sectional area in oropharynx; MDCT, multidetector computed tomography; NA, not available; NAV, nasopharyngeal airway volume; OAV, oropharyngeal airway volume; TOH, total oropharynx height.

**Table 13.** Extended

NAV			OAV			HAV			MCA		
Estimated value	Standard error	P value	Estimated value	Standard error	P value	Estimated value	Standard error	P value	Estimated value	Standard error	P value
6909.380	442.930	<.001*	28213.80	1989.580	<.001*	7088.471	373.562	<.001*	225.717	14.548	<.001*
-834.300	417.600	.047*	-7257.00	1875.790	<.001*	-2292.29	339.470	<.001*	-79.467	13.716	<.001*
-1125.52	417.600	.008*	180.570	1875.790	.042*	-903.139	379.539	.018*	59.283	13.716	<.001*
NA	NA	NA									
-139.800	511.450	.785	60.530	2297.370	.979	55.906	402.562	.890	1.45	16.798	.931
-154.100	511.450	.763	58.180	2297.370	.980	75.406	402.562	.852	1.7	16.798	.920
-92.130	511.450	.857	-95.820	2297.370	.967	-81.594	402.562	.840	3.05	16.798	.856
-114.070	511.450	.824	16.030	2297.370	.994	-0.563	402.562	.999	-0.975	16.798	.954
-29.700	511.450	.954	-94.670	2297.370	.967	22.188	402.562	.956	0.175	16.798	.992
814.000	590.570	.169	-1998.12	2652.770	.452	396.006	480.084	.411	-37.6	19.397	.050*
NA	NA	NA									
NA	NA	NA									

Downloaded from https://prime-pdf-watermark.prime-prod.pubfactory.com/ at 2025-07-01 via free access